

PROPOSAL FOR A LINAC-BASED RHIC PREINJECTOR

TABLE OF CONTENTS

Summary

1. Introduction

- 1.1 Acceleration scheme, nominal intensities and efficiencies
- 1.2 Features and advantages of the new preinjector
- 1.3 The EBIS Source

2. Results of the EBIS Test Stand

- 2.1 Demonstration of high current electron beam formation and propagation
- 2.2 Extraction of ions from the EBTS trap
- 2.3 Fast extraction of ions from the EBTS trap
- 2.4 Measurement of charge state distribution of ions from EBTS
- 2.5 Additional EBTS results
- 2.6 Summary of EBTS Performance

3. Design of the new preinjector

- 3.1 Features of an EBIS for RHIC
 - 3.1.1 Electron gun
 - 3.1.2 Electron collector
 - 3.1.2.1 Capacity of the electron collector to dissipate the power of the electron beam
 - 3.1.2.2. Collector Optics
 - 3.1.2.3. Mechanical design of the collector
 - 3.1.2.4 EBIS Electron Collector Cooling System
 - 3.1.3 Superconducting Solenoid
 - 3.1.4 EBIS vacuum system
 - 3.1.4.1 Vacuum requirements for the ionization region
 - 3.1.4.2 Requirements to the vacuum system
 - 3.1.4.3 Structure of the RHIC EBIS vacuum system
 - 3.1.5 Seeding the EBIS trap
 - 3.1.6 EBIS Power Supply Requirements
 - 3.1.7 EBIS Controls and Timing
- 3.2 LEBT
- 3.3 RFQ
 - 3.3.1 Choice of Parameters
 - 3.3.2 Specifications
 - 3.3.3 Beam Dynamics
- 3.4 MEBT

- 3.5 IH Linac
 - 3.5.1 Specification of Parameters
 - 3.5.2 Beam Dynamics
- 3.6 HEBT
- 3.7 Diagnostics and Controls
- 3.8 RF Systems
- 3.9 Vacuum systems
- 3.10 RFQ & linac water system

4. Booster Injection with the EBIS Beam

- 4.1 EBIS Beam
- 4.2 Space Charge Effect
- 4.3 Longitudinal aspects
 - 4.3.1 Capture of unbunched beam
 - 4.3.2 Capture of bunched beam
- 4.4 Inflector Aperture Limit and Scraping Effect

5. Facility Modifications

6. ESHQ and Waste Management

References

Appendix 1 Parameter List

PROPOSAL FOR A LINAC-BASED RHIC PREINJECTOR

Summary

This proposal describes a new heavy ion preinjector for RHIC based on a high charge state Electron Beam Ion Source (EBIS), a Radio Frequency Quadrupole (RFQ) accelerator, and a short Linac. The highly successful development of an EBIS at BNL now makes it possible to replace the present preinjector that is based on an electrostatic Tandem with a reliable, low maintenance Linac-based preinjector. Linac-based preinjectors are presently used at most accelerator and collider facilities with the exception of RHIC, where the required gold beam intensities could only be met with a Tandem until the recent EBIS development. EBIS produces high charge state ions directly eliminating the need for the two stripping foils presently used with the Tandem. Unstable stripping efficiencies of these foils is a significant source of luminosity degradation in RHIC. The high reliability and flexibility of the new Linac-based preinjector will lead to increased integrated luminosity at RHIC and is an essential component for the long-term success of the RHIC facility. This new pre-injector, based on an EBIS, also has the potential for significant future intensity increases and can produce heavy ion beams of all species including uranium beams and could also be used to produce polarized ^3He beams. These capabilities will be critical to the future luminosity upgrades and electron-ion collisions in RHIC.

The new RFQ and linac that are used to accelerate beams from the EBIS to an energy sufficient for injection into the Booster are both very similar to existing devices already in operation at other facilities. Injection into the Booster will occur at the same location as the existing injection from the Tandem.

1 Introduction

The present preinjector for heavy ions for AGS/RHIC uses the Tandem Van de Graaff, built around 1970. The beam is transported to the Booster via an 860 m long line, as shown schematically in Figure 1.1.1. The proposed replacement consists of an Electron Beam Ion Source (EBIS), followed by a Radio Frequency Quadrupole (RFQ) accelerator, and a short Linac. This new preinjector offers improvements in both performance and operational simplicity, as described below.

The present state of EBIS development is discussed in Chapter 2. In Chapter 3 the design of the new preinjector is presented, including features of the EBIS for RHIC, and details of the following acceleration stages. A description of injection into the Booster is given in Chapter 4.

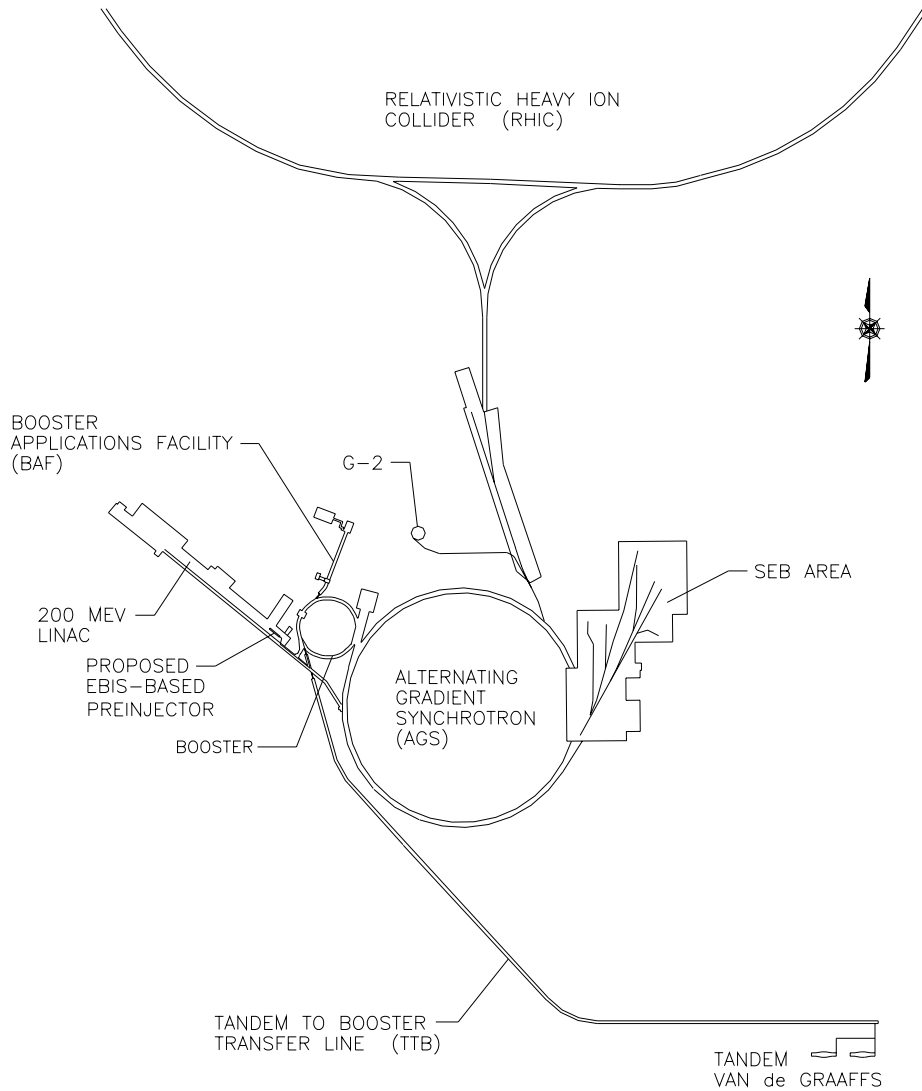


Fig. 1.1.1 Schematic of the present Tandem injection and future EBIS injection lines.

1.1 Acceleration scheme, nominal intensities and efficiencies

The present scheme for filling RHIC uses one ion source pulse (and one Booster pulse) to fill one bunch in RHIC. Using Au as the most common example, for the required 10^9 ions per bunch in RHIC, and with a transfer efficiency of about 50% (including stripping after the Booster) from Booster to AGS (and RHIC), one needs to achieve 2×10^9 Au ions per pulse extracted from the Booster.

Present heavy ion injection into the Booster from the Tandem Van de Graaff starts with a sputter negative ion source on a 150 kV high voltage platform, which can deliver approximately $200 \mu\text{A}$ of Au^- in $500 \mu\text{s}$ pulses. The beam is then accelerated to the 14 MV terminal, where ions are stripped by passage through a $2 \mu\text{g}/\text{cm}^2$ carbon foil, and then accelerated to ground potential, where the total current (all charge states) is $\sim 1 \text{ e mA}$, with approximately 20% of that being in the desired 12^+ charge state. At ground,

the beam then passes through a second carbon stripper foil, with $\sim 70 \text{ e}\mu\text{A}$ in the desired Au^{32+} charge state, with an energy of about 0.92 MeV/amu. This beam is transported 860 m to the Booster, where it is injected over ~ 35 turns, with a capture efficiency of about 50%.

An attractive alternative scheme is to produce, directly from an ion source, the charge state desired for Booster injection. This eliminates the inefficiencies due to stripping, and makes the initial preacceleration more efficient. In addition, Booster injection is more efficient if one can inject over fewer turns, so it is also desirable for the source to produce shorter pulses of higher currents. Some of the parameters required from a new preinjector are listed as follows:

1. **Intensity at injection into the Booster: $2.7 \times 10^9 \text{ Au}^{32+}$ ions per pulse.** Sufficient to achieve 1×10^9 ions per bunch in RHIC.
2. **Injected pulse width: variable, 10 – 40 μs .** This allows 1-4 turn injection into the Booster. This simplifies the injection, and should greatly reduce the sensitivity to small beam losses at injection, which may cause a pressure bump resulting in further beam loss.
3. **Repetition rate: 5-10 Hz.** This keeps overall RHIC fill times to only a few minutes
4. **Injection energy: 2 MeV/amu.** Present tandem injection is at 0.92 MeV/amu for Au. At this energy, there is a significant beam loss due to electron capture during Booster injection. By raising the injection energy to 2 MeV/amu, the capture cross section is reduced by a factor of 20-40. In addition, the higher energy reduces the space charge tune shift at injection, which might be important at these higher peak currents. At even higher injection energies one would approach the voltage limit of the inflector, and losses due to ionization would begin to become important.
5. **Q/m: 0.16 or greater.** This ratio equals that presently delivered for Au from the tandem. For lighter ions, the higher q/m is required (Si^{14+} , Fe^{21+}) to achieve the desired Booster output energy, within rigidity constraints in the Booster and extraction transport.
6. **Emittance (90%, unnormalized): $11 \pi \text{ mm mrad}$ or less.** Matches the acceptance of the inflector with minimal losses. This emittance is acceptable for the few-turn injection, but if one were to inject over 10^3 's of turns, as with the tandem, the emittance requirement is stricter.
7. **dp/p : 0.05% or less.**

These parameters can be achieved with an EBIS source, followed by an RFQ and short linac. A schematic of the injection scheme with the new injector is shown in Fig. 1.1.2. A detailed parameter list for the injector is given in Appendix 1.

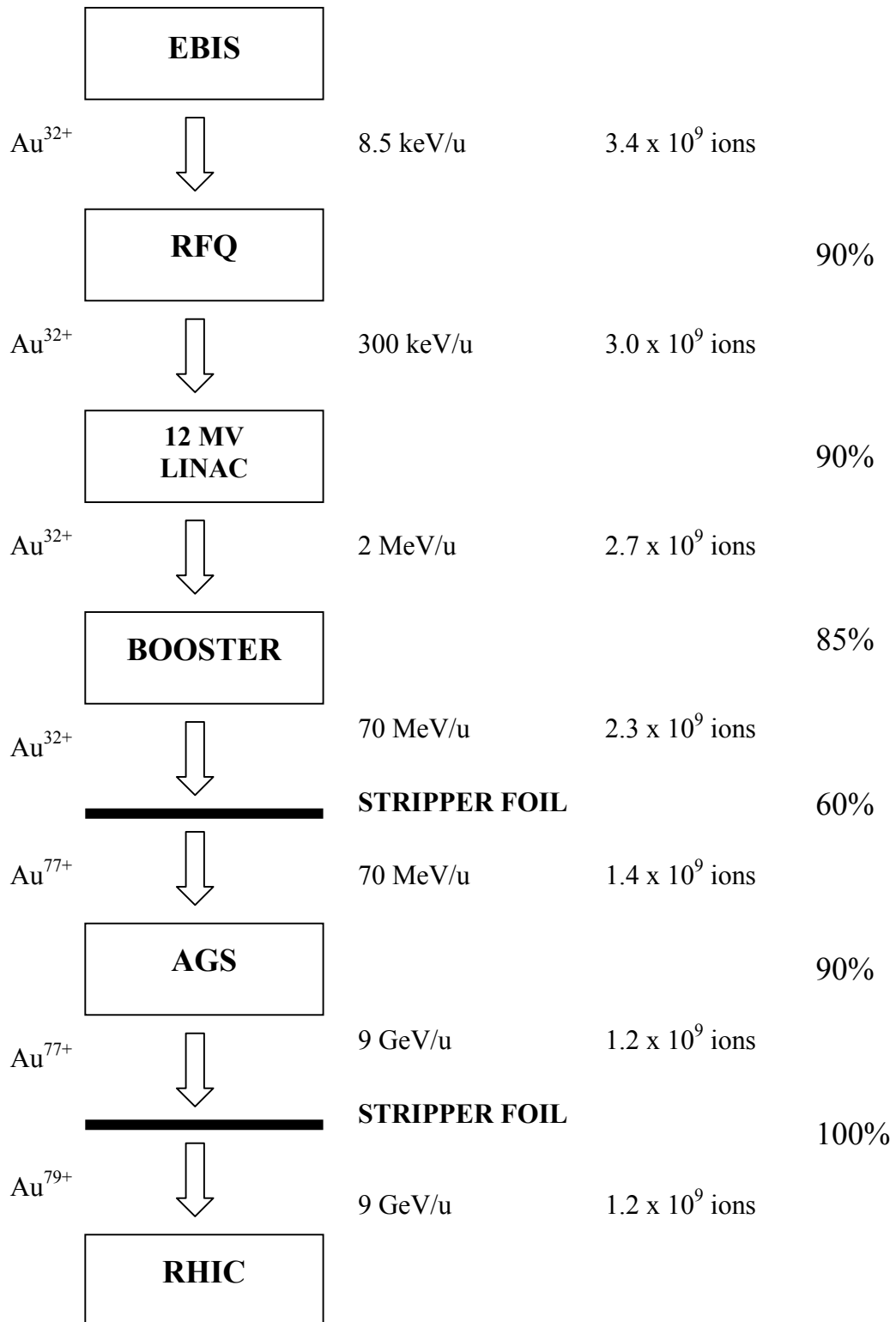


Fig. 1.1.2 Schematic of linac-based injection, showing ions per pulse, and efficiencies at various stages.

1.2 Features and advantages of the new preinjector

Linac-based preinjectors are presently used at most accelerator and collider facilities with the exception of RHIC, where the required gold beam intensities could only be met with a Tandem until the recent EBIS development. The high reliability and flexibility of a new Linac-based preinjector will be an essential component for the long-term success of the RHIC facility. The Linac-based preinjector offers the following advantages:

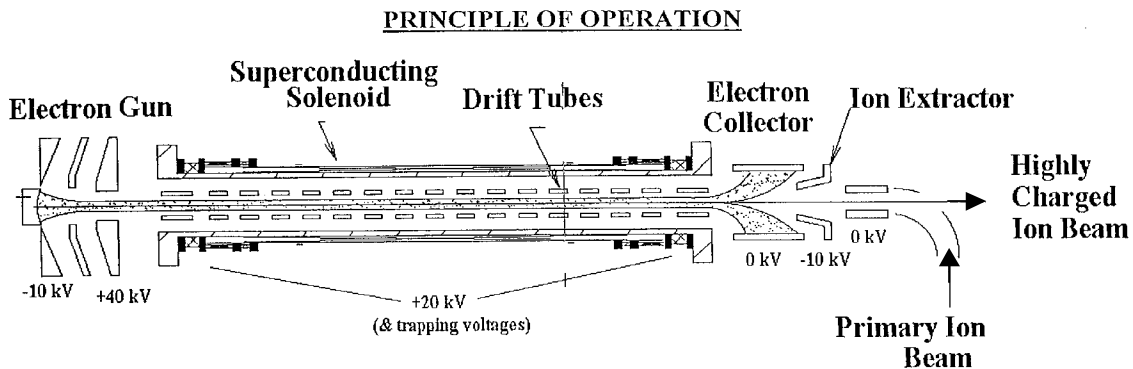
- While the Tandem has proven to be reliable, quite a few systems are becoming obsolete, and would have to be replaced to maintain reliable long term operation for RHIC. The RFQ and linac are a simpler, modern, more robust technology, which will require less maintenance. This is similar to our very favorable experience of replacing a large electrostatic device, the Cockcroft –Walton preaccelerator, with a compact RFQ accelerator for H^- ions in the 200 MeV linac. In that case, one went from a device that occupied one person full time with maintenance, to the RFQ, which requires almost no maintenance and has had almost no downtime over its 10 years of operation.
- The Tandem requires stripping foils at two locations. Although foil lifetime should become less of an issue as RHIC beam storage times increase, the energy spread in the Tandem beam changes as the foils age (thicken). The EBIS requires no stripping before the Booster.
- The 860 m long Tandem-to-Booster transport is difficult to tune, especially when changing the species. The new line will be only about 30 m long, and will use a more stable FODO lattice.
- The EBIS will inject only 1-4 turns, as opposed to 30-40 from Tandem, so injection will be much easier.
- The higher Booster injection energy will reduce losses at injection.
- Tandem species are limited to ions starting as negatives, while the EBIS can produce all ions.
- The EBIS can switch species very quickly, for filling RHIC with two different ions, or for fast switching between RHIC and the Booster Application Facility (BAF). Fast switching with the Tandem requires the use of the two BNL Tandems.

With the long-term commitment to heavy ions at BNL for RHIC, and increasing demands for different species and delivery of beams to different users, the EBIS preinjector will enhance capabilities significantly. Undoubtedly, additional unexpected impacts of the EBIS preinjector will appear as one gains experience and explores the new parameter space it will present. Even with a new preinjector, one can imagine that the Tandem will continue to play an important role. Multiple injectors are not uncommon at heavy ion facilities since the preinjectors are a relatively low-cost, high impact part of a facility.

1.3 The EBIS Source

The principle of operation of an Electron Beam Ion Source is shown schematically in Fig. 1.3.1. At one end an electron beam is produced, and then compressed to high density as it enters a strong solenoidal magnetic field. The beam passes through the solenoid, is decelerated, and then stopped in the electron collector. The EBIS trap region is a series of cylindrical electrodes in the main solenoid. Electrostatic barriers are produced on the ends of the trap region by applying positive voltages on the end electrodes. Ions are confined radially by the space charge of the electron beam. The trap is seeded either by injecting neutral gas of the desired species, or by axial injection and trapping of singly charged ions produced in an external ion source. As the ions are held in the trap, they are step-wise ionized, until the desired charge state is reached, at which time the voltage on one end electrode is reduced and the ions are extracted. They pass axially through the electron collector and into a beam transport line.

One essential feature of the EBIS is that it produces a narrow charge state distribution, with the charge state in the peak increasing as the product of electron beam current density and ion confinement time, $j_e \tau$, increases. It is therefore straightforward to achieve any desired charge state; this is especially the case for an EBIS for RHIC where the needed charge states are very modest. A second feature of EBIS is that it produces a fixed amount of positive charges per pulse. The number of trapped charges can increase only to the point where the space charge of the electron beam is neutralized. The maximum yield of positive charges therefore roughly equals the electron beam charge in the trap (trap capacity). Neutralization efficiency is the ratio of extracted ion charge to trap capacity, and is usually greater than 50%, but can be as high as 100%. As shown in the equation in Fig. 1.3.1, the yield of the desired charge state is the product of trap capacity, neutralization efficiency, and fraction in the desired charge state.



Yield of ions in charge state q :

$$N_q = \frac{I_e \times L}{q \times \sqrt{V_e}} \times K_1 \times K_2$$

I_e =electron beam current
 K_1 =neutralization factor

V_e =electron beam voltage
 K_2 =fraction in desired charge state

L =trap length

Fig. 1.3.1 Principle of EBIS Operation

An EBIS delivers pulses having a constant total positive charge, and one has control over the ion pulse width by controlling the release of the trap voltage. Ions can be extracted in short pulses of high current, which is desirable for synchrotron injection. With the properties of an EBIS being well understood, one can arrive at design parameters for an EBIS meeting RHIC requirements. These parameters are given in Table 1.3.1. While this combination of parameters is not unique, based on past and present experience we feel that they represent the most straightforward path to the design goals. Also given in the table are some of the presently achieved parameters from the BNL EBIS test stand (EBTS).

Table 1.3.1 EBIS Parameters

Parameter	RHIC EBIS	EBTS (achieved to date)
e-beam current	10 A	10 A
e-beam energy	20 keV	20 keV
e-beam density	$\sim 575 \text{ A/cm}^2$	$> 575 \text{ A/cm}^2$
Ion trap length	1.5 m	0.7 m (solenoid limit)
Trap capacity (charges)	11×10^{11}	5.1×10^{11} (10A)
Yield positive charges	5.5×10^{11} (Au, 10 A)	3.4×10^{11} (Au, 8 A)
Pulse length	$\leq 40 \mu\text{s}$	20 μs
Yield Au ³²⁺ , design value	3.4×10^9 ions/pulse	$> 1.5 \times 10^9$ ions/pulse

The electron beam neutralization efficiency for RHIC EBIS is assumed to be 50%, a value that has been consistently exceeded on our EBTS, as well as in many other EBISs. The yield in the desired charge state is assumed to be 20%, again a value which is frequently achieved in EBISs.

We have also considered other sources for the production of pulsed currents of intermediate charge state ions for synchrotron injection – specifically the Electron Cyclotron Resonance (ECR) ion source, and the Laser Ion Source (LIS). These sources have a more difficult time achieving the desired charge state, so while with an EBIS one is using the peak charge state from a narrow distribution, with the ECR and LIS one is typically using a charge state on the tail of a much broader distribution. Thus, for the same current in the desired charge state, one has to deal with much higher total extracted currents, and their accompanying problems of transport and matching into the RFQ of these higher total currents. For example, 3.4×10^9 Au³²⁺ ions in a 10 μs pulse corresponds to a Au³²⁺ current of 1.7 mA. The total extracted current from the EBIS will be 8.5 mA, assuming 20% in the desired charge state. For the same Au³²⁺ currents, total current from an ECR or LIS could be up to 10 times higher (this is considerably above what an ECR has achieved). If one goes to a lower charge state from the ion source, then in addition to the accelerator becoming longer, the total current required becomes even higher because an additional stripping would be required after acceleration.

Both sources also have some limitations in the ions that can be produced, the LIS requiring high melting point solids, and the ECR having difficulty producing ions from high melting point solids. The LIS has additional obstacles, such as large emittance due to a large energy spread, target erosion and coating of mirrors, state of the art laser required, and very large pulse-to-pulse fluctuations in beam current.

Unlike these two sources, an EBIS can easily produce any type ions – from gas, metals, etc., and can quickly switch species (even pulse-to-pulse) without a memory effect. One can easily control the width of the extracted pulse. Scaling laws for EBIS are well understood, and the source is reliable, with excellent pulse-to-pulse stability.

2 Results of the EBIS Test Stand

The requirements for the RHIC EBIS were given in Table 1.3.1. These parameters were considerably beyond the previous state of the art, since most EBIS sources were designed for atomic physics applications, where much lower intensities of very high charge state ions were usually desired. The most recent phase of the BNL EBIS development program has been to demonstrate that an EBIS capable of meeting the RHIC requirements can be built. Our approach has been to construct a full power close to 1/2 length prototype, show that each subsystem can work, demonstrate ion production and extraction in expected quantities, and finally demonstrate the production of heavy ions with $q/A \sim 0.16$ centered in a narrow charge state distribution. With this EBIS Test Stand (EBTS), we have been able to develop many of the relevant technologies, and study the physics aspects of a high intensity EBIS. A number of issues have been addressed, among them the technology of high current electron beam formation and launching, development of primary ion injection into the trap, the study of ion formation in and loss from a high current electron beam, the study of fast ion extraction, and the development of appropriate source controls and diagnostics. There are some practical aspects in the present design that limit the performance of EBTS, such as the power handling limit of the electron collector, the electron collector power supply, (a 25 year old supply that had been out of service for 15 years), and power supply and design limits to voltages which can be applied to various trap electrodes. The EBTS is shown schematically in Fig. 2.1. A photo of the source is shown in Fig. 2.2. A schematic for ion extraction, transport, external ion injection, and diagnostics is shown in Fig. 2.3.

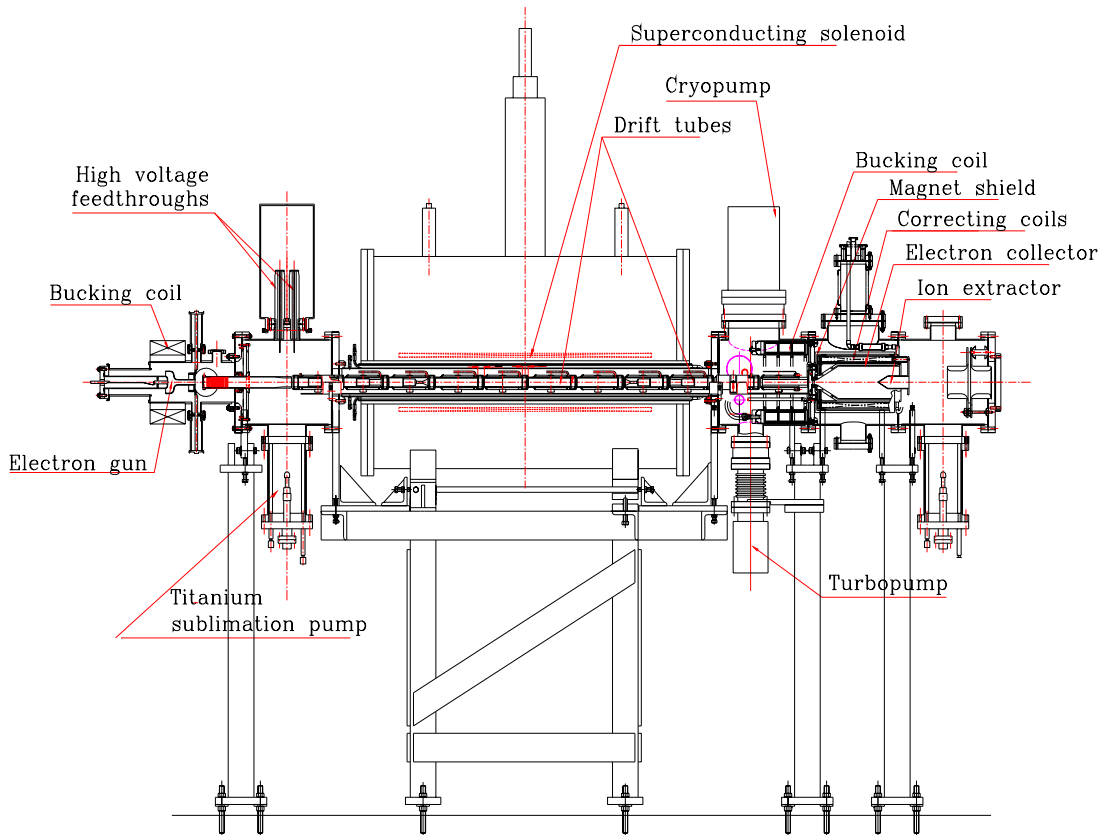


Fig. 2.1 Schematic of the EBIS Test Stand (EBTS).



Fig. 2.2 Photograph of EBTS

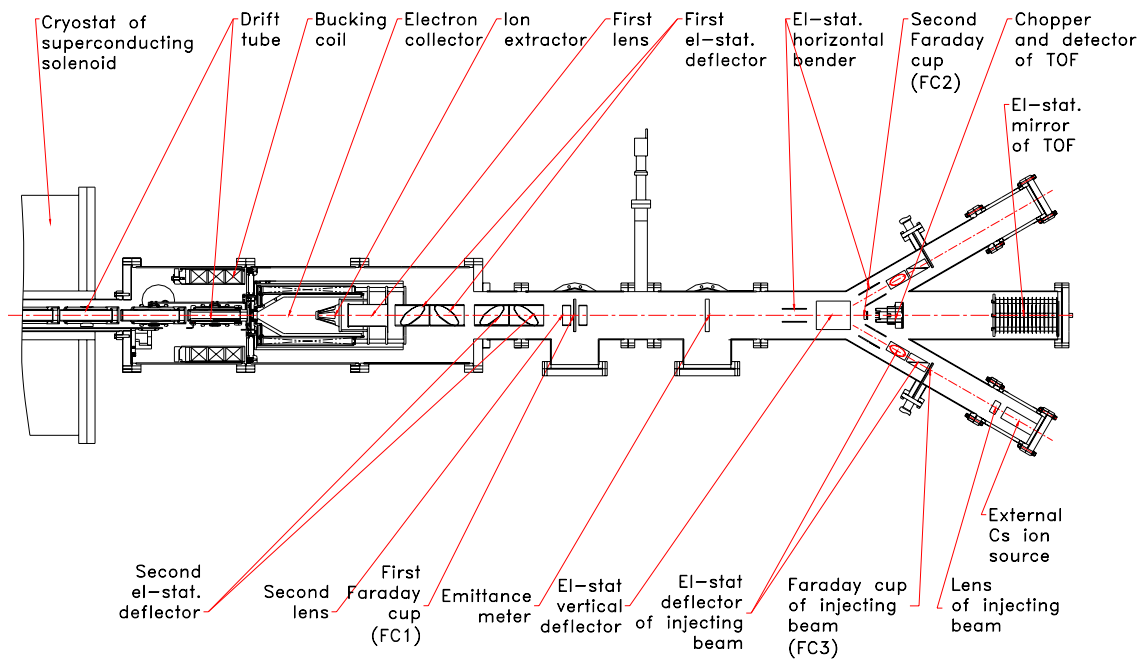


Fig. 2.3 Schematic of the ion extraction, transport, diagnostics, and external injector

Table 2.1 Key hardware features of the EBTS

Superconducting solenoid:	
Length	1 meter
Maximum field	5 Tesla
Bore	155 mm diameter, warm
Helium consumption	0.12 l/hr
Drift tubes	
No. of electrodes	12
Bore diameter	31 mm
Trap length	0.7 m
Electron gun cathode	LaB ₆ , 8.3 mm diameter
Electron collector power	50 kW
Vacuum	1×10^{-9} to 4×10^{-10} Torr in most regions (most sections bakeable to 200C, central DT's to 450 C)
Diagnostics	
Time-of-flight	Mamyrin-type, 2 m from ion extractor
Faraday cups	0.5 and 1.5 m from ion extractor
Harp	1.6 m from ion extractor
Emittance	1.6 m from ion extractor (under development)

Details of the EBTS design and experimental results have been presented in references [2-1] – [2-9]. Table 2.1 gives some parameters for the test stand. Some of the key achievements will be mentioned in the following discussion.

2.1 Demonstration of high current electron beam formation and propagation

The 10 A electron beam current required to reach ion beam yields for RHIC was an order of magnitude higher than achieved in any previous EBIS. The design of the electron gun was of crucial importance not only because of the requirement for such a high current, but also because of the need for a flexible control of the electron beam parameters. After performing an extensive study of different electron gun geometries it was decided to adopt a coaxial diode with magnetic insulation, positioned in the field of a separate solenoid (Fig. 2.1.1). The novel spherical convex LaB₆ cathode has a radius of curvature of 10.6 mm and transverse diameter of 8.3 mm. A photo of the gun cathode assembly is shown in Fig. 2.1.2. The gun was designed and fabricated at the Budker Institute of Nuclear Physics, Novosibirsk [2-5].

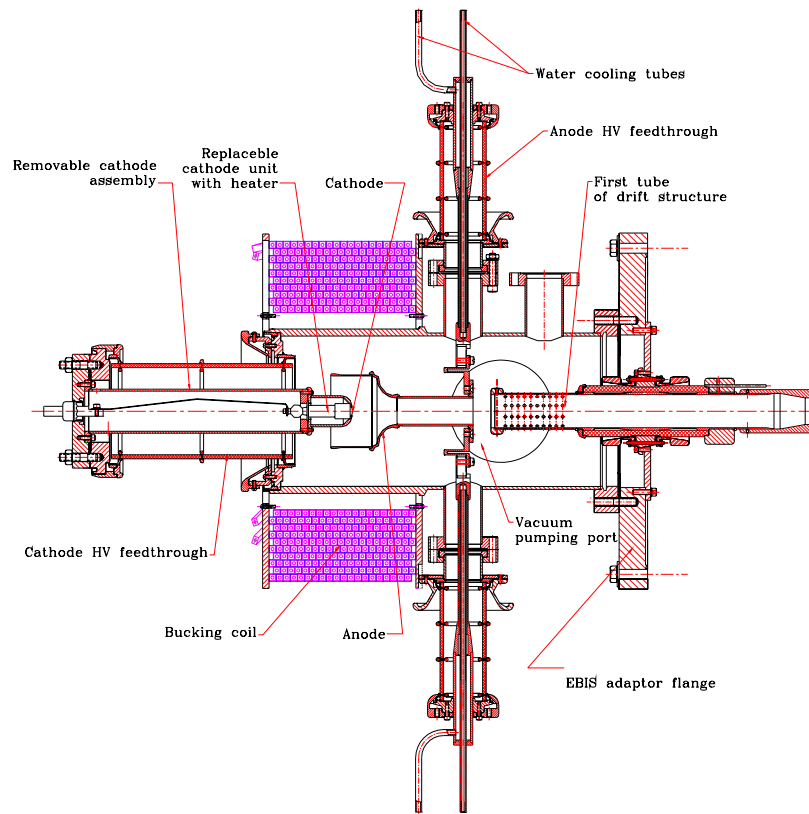


Figure 2.1.1 Electron Gun Assembly



Figure 2.1.1 Photo of the electron gun cathode assembly

The performance of this novel electron gun has been excellent. It has provided very stable operation over a wide range of gun operating parameters, with very satisfactory lifetime and reliability. With this gun we have reached our design goal, and propagated a 10 A electron beam through the EBIS solenoid to the collector, with very low beam loss (<0.5%), in ~50 ms pulses. Figures 2.1.3 and 2.1.4 show two examples of electron beam pulses propagating through the EBIS trap.

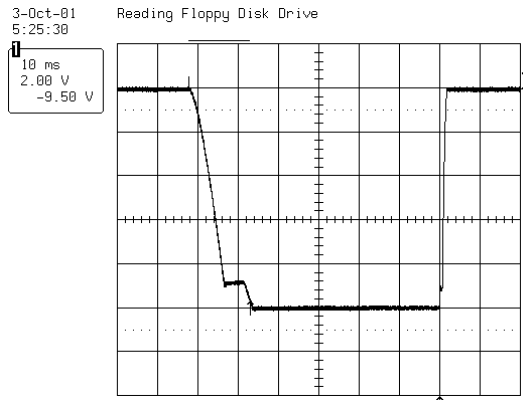


Fig. 2.1.3 10 A, 50 ms electron beam pulse.

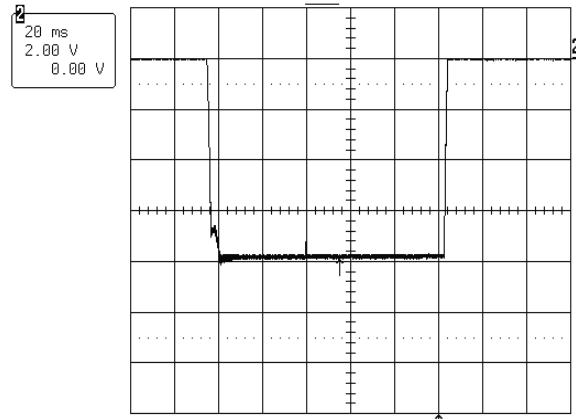


Fig. 2.1.4 8 A, 100 ms electron beam pulse.

2.2 Extraction of ions from the EBTS trap

Our design goal of extraction of the total ion charge corresponding to 50% of the electron beam space charge has consistently been met or exceeded. Trapping and ionization with continuous injection of Xe gas into the EBTS demonstrated good operation as a first test, although EBTS was not designed for gas injection. Subsequently, we have achieved excellent operation with Au, Cs, and Ta ions. In these cases, low charged ions were produced in an external ion source, and then injected into the EBIS trap for ionization to much higher charge states. Table 2.2.1 shows some ion yields under various operating conditions. The RHIC EBIS requires 5×10^{11} charges/pulse, at 10 A but with slightly over twice the trap length of EBTS.

Table 2.2.1 Ion yields from EBTS

Ion	Electron current	Ion yield charges/pulse	Neutralization
Gold	8.0 A	3.4×10^{11}	85 %
Xenon	7.0 A	1.9×10^{11}	55 %

We have not yet measured ion yields at the full electron beam current due to power supply limitations.

Figure 2.2.1 shows how EBTS ion yield has scaled properly with electron beam current. Also shown is the design goal for EBTS, i.e. achieving 47% of the RHIC requirement from 47% of the trap length.

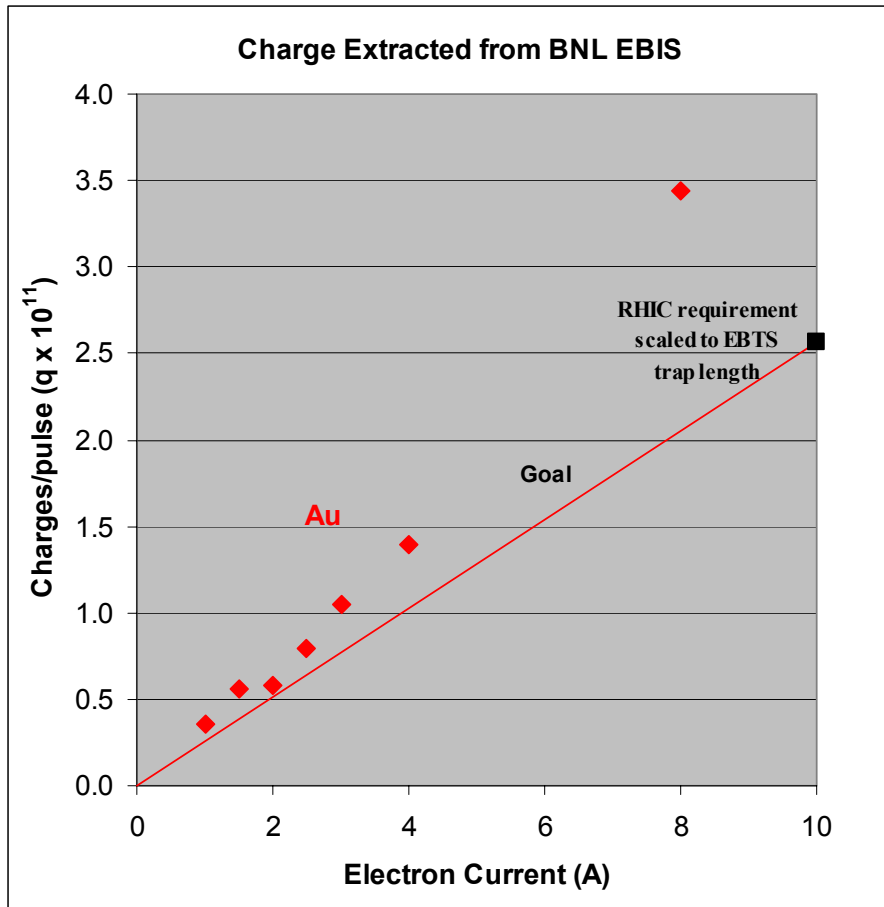


Fig. 2.2.1 Extracted ion charge as a function of electron current for EBTS.

2.3 Fast extraction of ions from the EBTS trap

For 1-4 turn injection into the Booster, the extracted ion pulse should be 10-40 μs long. Figure 2.3.1 is a 10 μs FWHM ion pulse extracted from EBTS, demonstrating that this requirement can be met at a high electron beam current (6 A in this case). This result was achieved by raising the voltage of the trap region above the level of the barrier electrode, with an additional voltage tilt in the trap produced via a fixed resistor/capacitor RC network. In a RHIC EBIS, with programmable control of electrode voltages, and an adjustable RC network, the shape and duration of the pulse will be controllable. The peak current of 3.3 mA is a record result for an EBIS. While this result shows ions produced from background gas, this fast extraction can be similarly achieved for any ions. For example, a 3.2mA, 12 μs FWHM, (40nC) ion pulse was obtained at the source exit toroid using a 6.8 A e-beam and Au external ion injection, after a 15ms confinement period, as shown in Fig. 2.3.2

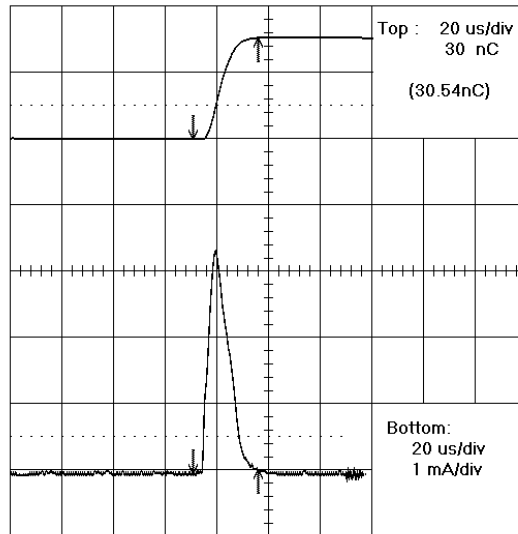


Figure 2.3.1: Bottom trace: 3.3 mA, 10 μs ion pulse extracted from the EBIS with a 6A, 17.6 kV electron beam and 10ms confinement time. Top: Integral of bottom trace (30.5 nC)

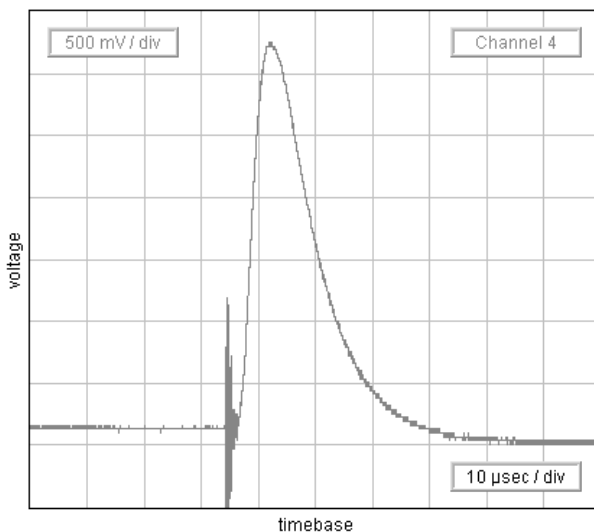


Figure 2.3.2: Total extracted current of 3.2mA, in 12 μs FWHM, with $I_e=6.8\text{A}$, Au injection, and 15ms confinement time.

2.4 Measurement of charge state distribution of ions from EBTS

Charge state distributions were measured on EBTS with a time-of-flight spectrometer located 1.5 m from the ion extraction electrode. Initially, distributions were measured using both Ar and Xe gas injection; an example of a Xe spectrum is shown in Fig. 2.4.1. The spectrum is peaked at Xe^{20+} ($q/m=0.15$), after 20 ms confinement with a 4 A electron beam.

The lower charge state tail on Fig. 2.4.1 is typical of continuous gas injection. Narrower charge state distributions have been demonstrated on EBISs such as those in Stockholm and Saclay using injection of singly charged ions from an external source into the trap. In EBTS, we have reached this major milestone by injecting ions from external sources for ions of Cs^{1+} , Ta^{1+} , and Au^{1+} . These ions were transported ~ 2 m to the EBIS, where they were trapped and further ionized. This external injection was very successful. Fig. 2.4.2 shows a narrow gold charge state distribution, with the desired 20% of the gold ions in a single charge state. Contaminant peaks will presumably be reduced with improved baking of the system. The peak charge state of Au^{33+} after only 40 ms confinement with an 8A electron beam already exceeds our requirement.

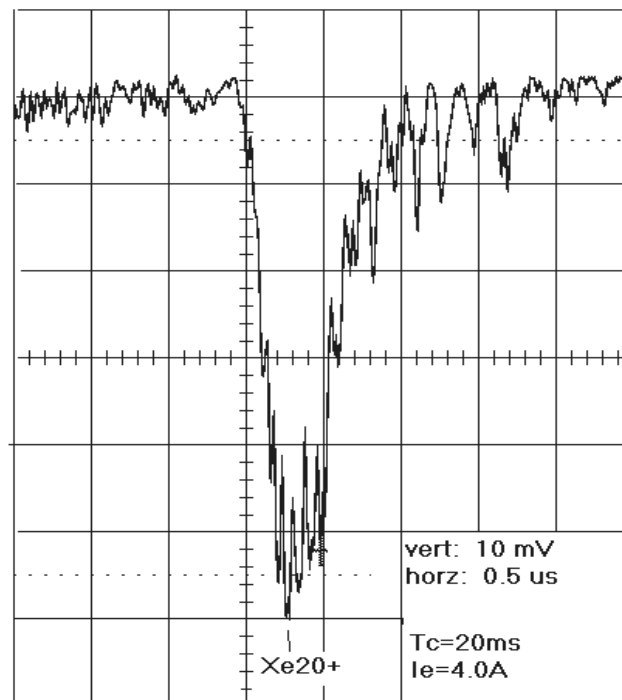


Fig. 2.4.1 Xe^{20+} produced using a 4A, electron beam and a confinement time of 20ms.

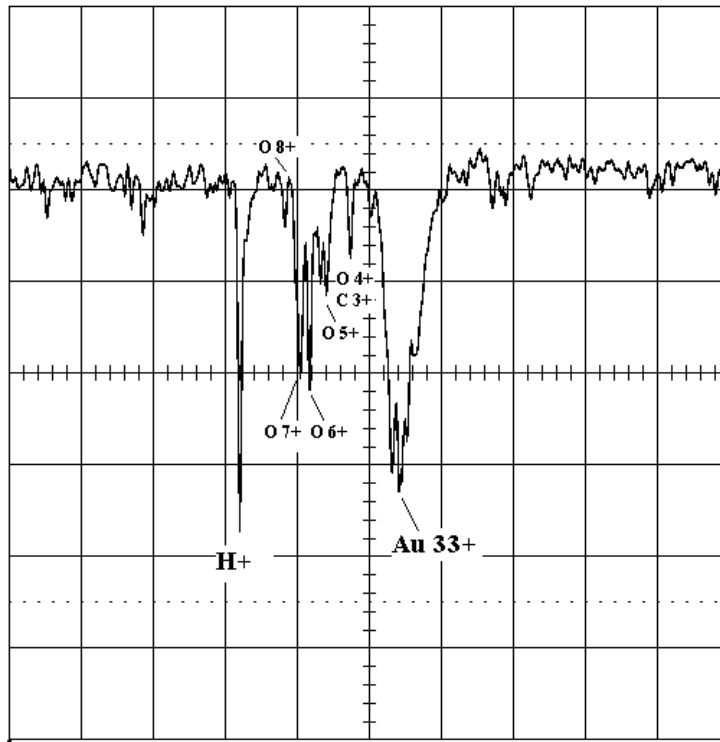


Fig. 2.4.2 Narrow Au charge state distribution coming from external gold ion injection into the EBTS ($I_e=7.2$ A, confinement time=40 ms).

2.5 Additional EBTS results

1. Trap length can be varied by changing the trap electrodes used to form the end barriers. Measurements of extracted ion yield as a function of trap length show the expected linear dependence.
2. Source performance has confirmed the advantages of a warm bore solenoid.
3. The design philosophy was correct with regard to vacuum requirements and to maintaining vacuum separation between regions of the source.
4. Good progress has been made regarding controls and fast voltage pulsing, allowing flexible programming of electrode voltages during the EBIS cycle.
5. The design incorporated transverse steering coils at all chamber locations, including the central drift tube region. These have proved to be extremely effective in optimizing electron beam transmission through the EBIS.
6. Preliminary emittance measurements were taken under a variety of source conditions, with a 6.8 A electron beam, extracted charge of 20-40 nC, and extracted currents of 1-3 mA. Normalized rms emittance values were typically measured to be in the range of 0.08–0.1 π mm mrad [2-9].

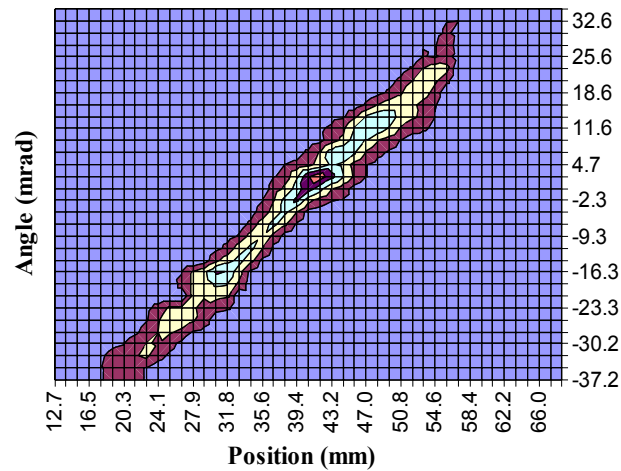


Figure 2.5.1: Emittance of a 1.7 mA extracted beam from EBIS, with Au injection. ϵ (n, rms) = 0.1π mm mrad.

2.6 Summary of EBTS Performance

- The EBTS is operating with parameters more than an order of magnitude above previous EBIS sources.
- We have achieved the design goal of transporting a 10 A electron beam through the 0.7 m EBTS trap with low losses.
- The extraction of Au ion pulses of 3.4×10^{11} charges with an 8A electron beam is less than a factor of 2 below the RHIC requirement for charge, and has demonstrated proper operation of an EBIS at high currents.
- The required Au charge state has been achieved with less than 40 ms confinement time.
- Ions have been extracted in pulses of amplitude 3.3mA and duration $\sim 10\mu\text{s}$ FWHM, which is important for meeting our goal of 1-4 turn injection into the AGS Booster ring.
- Au, Ta, and Cs ions from an auxiliary ion source were successfully injected into the trap of EBTS with a good efficiency.
- To date, all results of the EBTS have agreed with EBIS scaling laws, and continue to confirm the parameters for a RHIC EBIS that were presented approximately 10 years ago.

Practical constraints rather than physics issues have limited performance of the EBTS, and therefore, while the test stand will benefit from further design optimization, we are now confident that an EBIS can be scaled to meet RHIC requirements. This is discussed in the following section.

3. Design of the new preinjector

Some parameters of the preinjector are given in Table 3.1. The details of the subsystems are given in the following sections. A layout of the preinjector is shown in Fig. 3.1.

TABLE 3.1. Beam parameters of the proposed preinjector

EBIS			
	Output (single charge state)	1.1×10^{11}	charges
	Ion output (Au^{32+})	3.4×10^9	particles/pulse
	Pulse width	10 - 40	μs
	Max rep rate	10	Hz
	Beam current (single charge state)	1.7 - 0.42	mA
	Output energy	8.5	keV/amu
	Output emittance	0.35	π mm mrad, norm, 90%
RFQ			
	Q/m	0.16 - 0.5	
	Input energy	8.5	keV/amu
	Output energy	300	keV/amu
IH Linac			
	Q/m	0.16 - 0.5	
	Input energy	300	keV/amu
	Output energy	2000	keV/amu
Injection			
	# of turns injected	1-4	

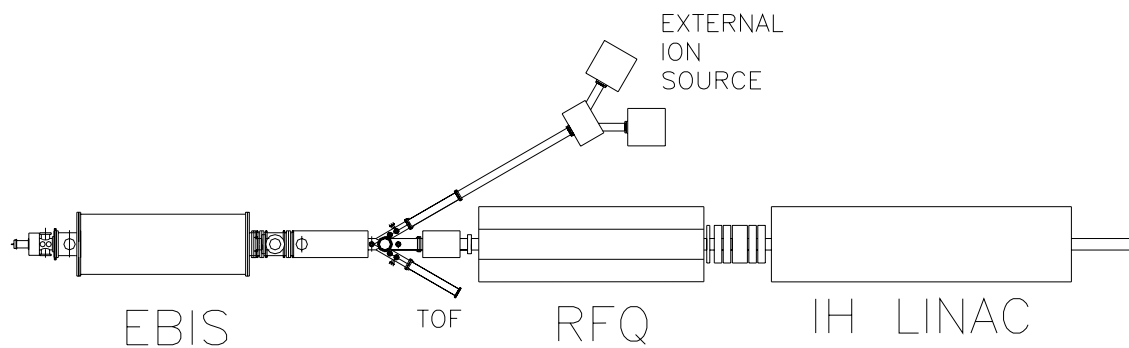


Fig. 3.1. Conceptual layout of the preinjector

3.1 Features of an EBIS for RHIC

Our experience so far in the operation of the EBTS has confirmed the validity of our approach to the design of the RHIC EBIS. New features we plan to incorporate into the final EBIS will be made in order to make the final EBIS more robust. A schematic of the RHIC EBIS is shown in Fig. 3.1.1. Presented below is our present concept for several key EBIS components. (Details may still change as a result of future EBTS R&D).

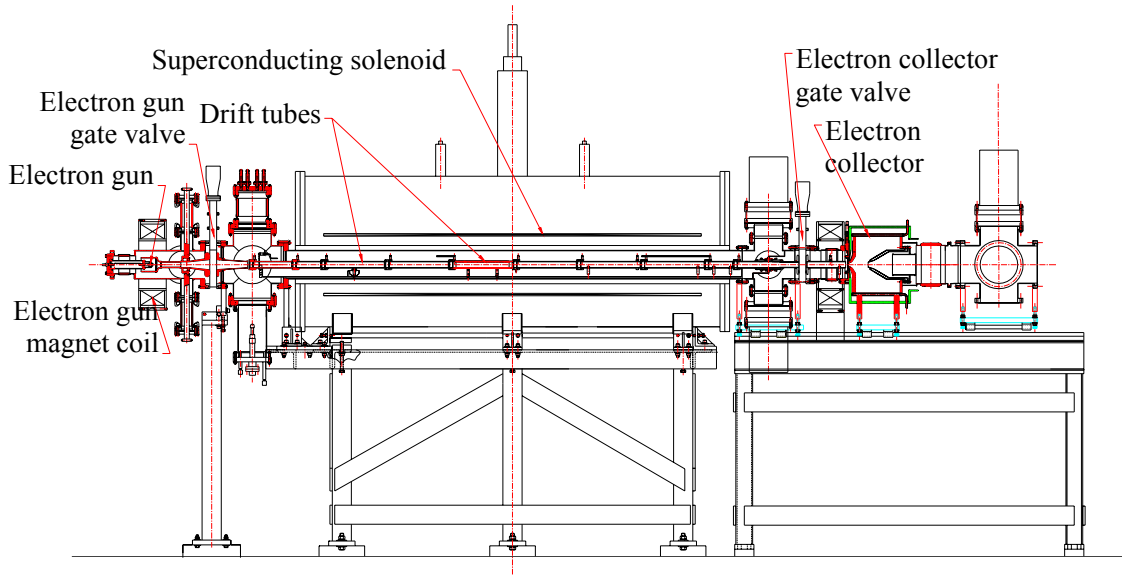


Fig. 3.1.1 Schematic of the proposed EBIS for RHIC.

3.1.1 Electron gun

As it has been mentioned previously, the required intensity of $\sim 3 \times 10^9$ of Au^{32+} ions per pulse can be provided with a trap containing $\sim 1 \times 10^{12}$ electrons. If the trap is 1.5m long and energy of electrons is 20 keV, the electron beam current should be 10 A. The microperveance of this electron beam is 3.5. There are several strict requirements to the electron beam, such as having the ability to strongly decelerate the beam in the strong magnetic field and in the collector region, and having the ability to operate over a wide parameter range. The existing electron gun with convex cathode and pure magnetic compression of the electron beam has proven to satisfy all our requirements.

The existing electron gun can generate an electron current of 10 A for 1000 hours, with an emission density of 13.5 A/cm^2 for 10 A electron beam. With further operation, the quality of electron beam becomes unsatisfactory due to deterioration of the cathode unit, and a simple replacement of the cathode is required. The existing unit meets our requirements, and it could be used for the RHIC EBIS. However, to have a more comfortable safety factor and a reserve for a possible future increase of the ion beam intensity, it would be advantageous to have an electron gun which is capable of generating an electron beam with a somewhat higher current, for example 15 A. To be able to extract an electron current in excess of 10A while at the same time increasing the lifetime of the gun, we plan to use a cathode unit based on IrCe rather than the present LaB_6 .

Published results of tests of IrCe cathodes show that even for an emission density as high as 30 A/cm² the lifetime is several thousands hours – much longer than we now have. A test of such a cathode on EBTS is planned for the near future. In collaboration with the Budker Institute of Nuclear Physics (BINP), additional improvements to the electron gun are being explored. The cathode unit design has been modified to reduce the heating power of the cathode and the surface area of the hot surfaces of the gun. The new electron gun will also have the anode water-cooled by heat conductance to reduce outgasing from the anode surface. BINP could again do detailed gun design and fabrication, as was the case for our 10 A gun.

To allow replacement of gun cathodes without exposing the rest of the EBIS to atmosphere, a gate valve between the gun and gun transition chamber will be installed. Simulations of the electron beam transmission demonstrate that the effect of adding a gap in the drift structure to accommodate the removable valve is negligible.

3.1.2 Electron collector

3.1.2.1 Capacity of the electron collector to dissipate the power of the electron beam

The main improvement in the new electron collector (EC) for the RHIC EBIS is an increase in its capacity to dissipate power, compared with the existing EC on the EBTS. The new EC will be designed to dissipate a power of 230 kW, which is 4.5 times higher than the existing EC, and 2.3 times higher than our expected load of 100 kW. In fact, the new EC will be able to dissipate the full power of a 15 A electron beam in DC mode. To increase the capacity of the EC, three approaches will be used – the peak power density at the cooling water channels will be reduced relative to the inner surface power density, the heat exchange by cooling water will be increased, and the pressure of the cooling water will be increased.

To reduce the maximum power density on the surface-water interface, the longitudinal distribution of the electron beam on this surface will be made more homogeneous than in the existing EC by optimizing the shape of the magnetic field. The total area of the cylindrical water-cooled surface of the EC will also be increased; with the new collector having an inner diameter of ~30 cm and a length of ~24 cm. The ratio of surface area of cooling channels to the area of inner EC cylindrical surface will also be increased. The flow rate of cooling water will be 4 GPM through a single channel, two times higher than in the existing EBTS. Raising the pressure of the cooling water to 25 bar increases its boiling temperature to 200 C, making possible a heat exchange without creating a vapor sheath on the surface for a local power density up to 700 W/cm². The main parameters of the new and existing EC are compared in Table 3.1.2.1.1.

Table 3.1.2.1.1 Parameters of the new and present electron collectors

Parameter	New EC	Existing EC
Design power dissipation, kW (actual beam power = 100 kW)	230	50
Area of inner cylindrical surface, cm ²	2200	1000
Maximum removable power density, W/cm ² (reduced area) (actual estimated max. pwr. density = 385 W/cm ²)	700	200
Water flow through the single channel, GPM	4	2
Diameter of the cooling channel, mm	8	6.4
Length of one cooling loop, m	2.6	1.8
Number of parallel cooling loops	10	4
Pressure drop of cooling water on channels, bar	5	2.7
Output pressure of cooling water, bar	20	1
Total water flow through all cooling channels, GPM	40	10.8
Diameter of entrance diaphragm, mm	23.9	17.8

3.1.2.2. Collector Optics

The electron beam transmission in the vicinity of the electron collector and its injection into the EC entrance diaphragm is controlled independent of the main solenoid field with an electron collector magnet coil located outside of the vacuum. The diameter of the electron collector entrance diaphragm is 16.8 mm, and is close to that of EBTS (17.8 mm). The optics of the electron beam in the new EC is made versatile, accepting the electron beam over a wide range of operating parameters (electron current, electron energy and magnetic compression). The ion optics through the new EC is optimized to achieve a larger acceptance of the ion beam; one will be able to extract ion currents up to 15 mA without losses on the EC or ion extractor. Electron trajectories in the new EC, simulated for an electron current of 15 A, are presented in Fig. 3.1.2.2.1.

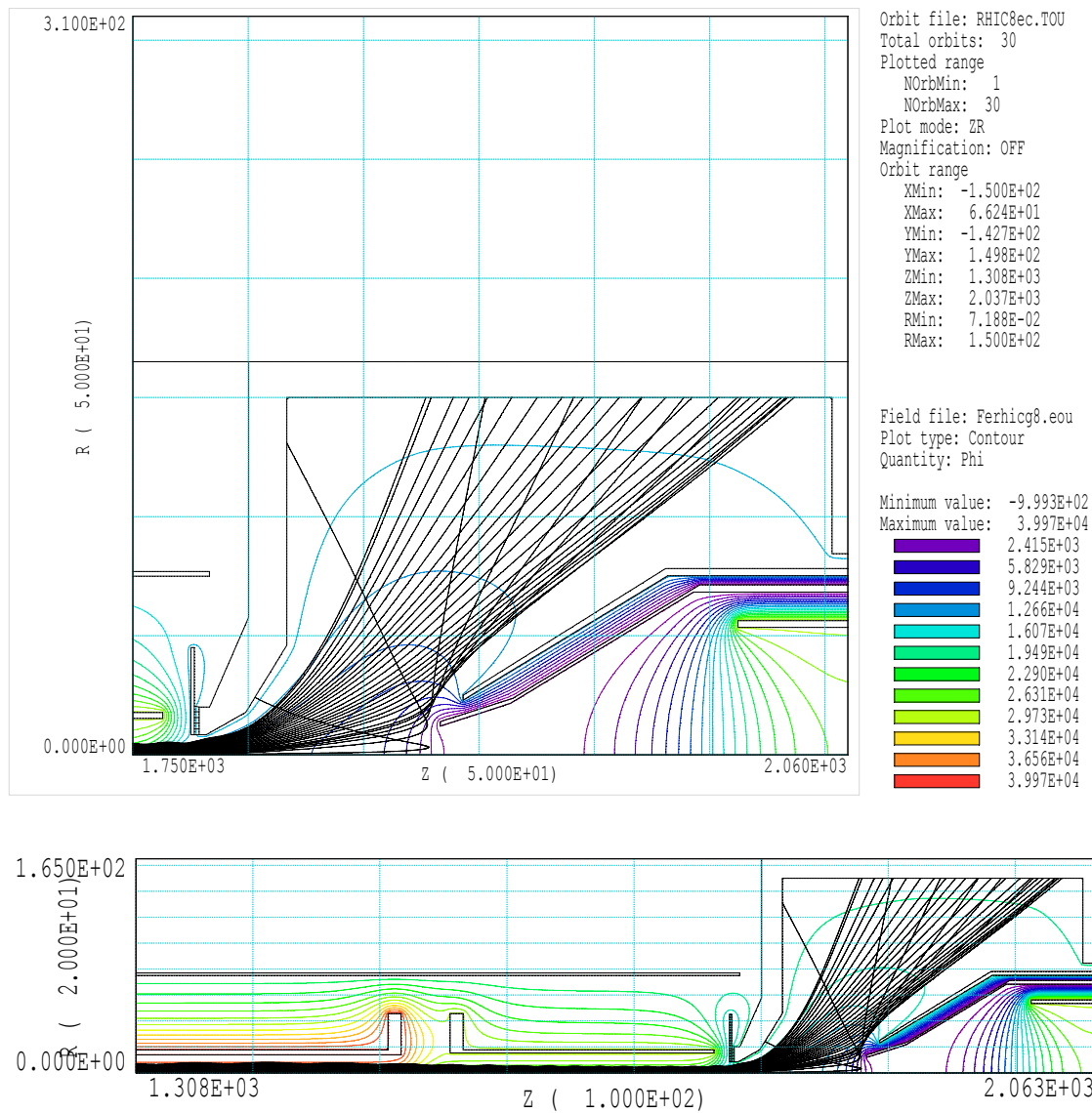


Fig. 3.1.2.2.1: Simulated trajectories of electron beam with current 15 A entering the electron collector with energy 15 keV.

3.1.2.3. Mechanical design of the collector

Unlike in the EBTS, the outer surface of the new EC will be exposed to atmosphere. This concept allows us to practically eliminate any probability of water leaks into the vacuum volume, because no water-cooling tubes will be in the vacuum. It also allows easy access to the EC body for monitoring power dissipation on the EC surface by measuring the temperature distribution on the outside surface. The concept of vacuum separation between the EC and central vacuum chamber, used in EBTS, will be preserved. The EC will be electrically isolated from other vacuum chambers with insulators capable of holding a DC voltage of up to 25 kV. The conceptual view of the EC assembly is presented in Fig. 3.1.2.3.1.

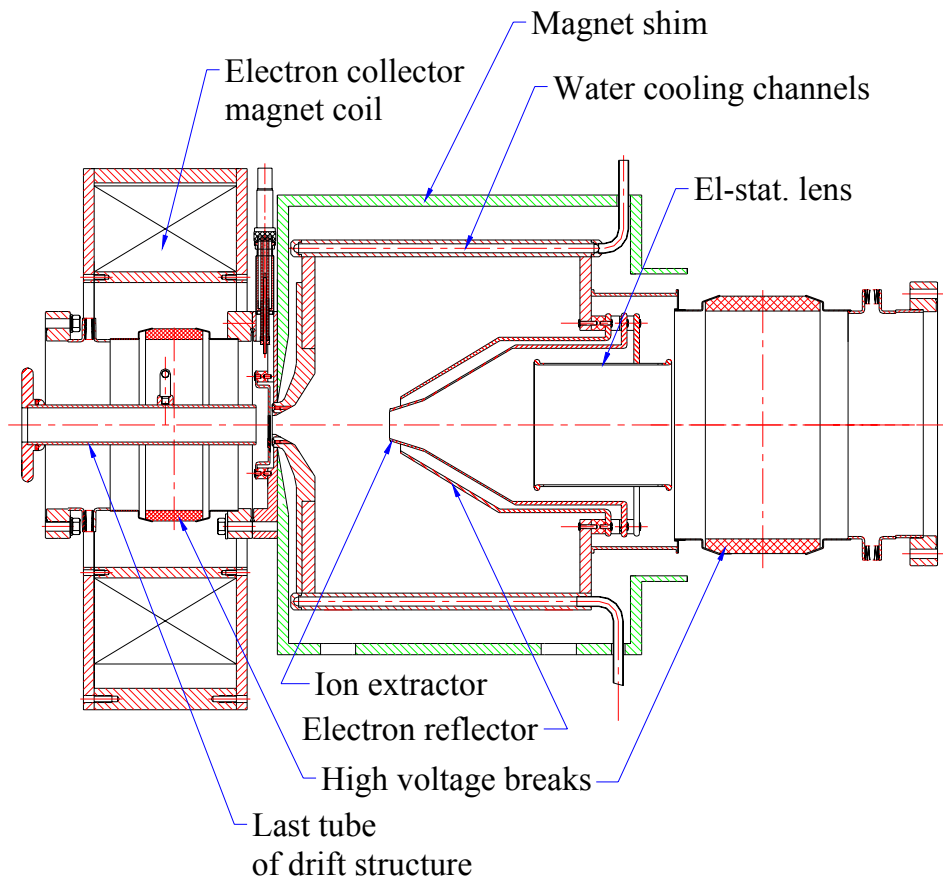


Fig. 3.1.2.3.1 Conceptual assembly drawing of the electron collector for RHIC EBIS.

3.1.2.4 EBIS Electron Collector Cooling System

As presently envisioned, the EBIS electron collector cooling system will dissipate heat from the collector by the flow of water at 25 bar pressure through cooling channels in the collector. The 25 bar water pressure serves to increase the boiling point of the cooling water to lower the chance of reaching critical heat flux or burnout, caused by formation of a vapor film. A pressurized expansion tank maintains the static pressure head. The cooling system capacity of 400kW exceeds with good safety margin the maximum heat load running the EBIS in a DC mode. A small cooling tower to dissipate heat will be provided. The 40 GPM flow rate produces turbulent flow in the cooling channels, promoting high Reynolds numbers and good convective heat transfer.

3.1.3 Superconducting Solenoid

Table 3.1.3.1 shows the parameters of the new solenoid, as well as the parameters of the existing EBTS solenoid. The coil for the new solenoid will be split into three independently adjustable regions (25%/50%/25% of length), to allow some flexibility in the shaping of the axial field. The diameter of the warm bore of the solenoid may be increased to facilitate pumping, and to provide more space to reduce the likelihood of high voltage breakdowns.

Table 3.1.3.1: Required parameters of the superconducting solenoid, as well present EBTS solenoid parameters

	RHIC EBIS	EBTS
Guaranteed maximum magnet field:	5 T (tested to 5.5 T)	5T (tested to 5.5)
Inner diameter of the warm bore	204 mm (clearance for 8" flange)	155 mm (clear for 6")
Total length of solenoid	2000 mm	1000 mm
Homogeneity over region 1300x10mm	0.25%	0.25%
Maximum radial shift of magnet field axis over full length of the magnet (documented)	0.2 mm	0.2 mm
Maximum radial deviation of position of solenoid axis from the position of warm bore axis	0.2 mm	0.2 mm
Decay rate of magnet field in coils of solenoid, operating with current leads removed.	1×10^{-6} per hour	1×10^{-5} per hour
Length of vacuum jacket	~ 2300 mm	1300 mm
Period between liquid helium refills	30 days	23 days
Period between liquid nitrogen refills	10 days	12 days

We have had initial discussions with staff at IHEP, who have expressed an interest in fabricating the solenoid. In addition, there is also a possibility that the Magnet Division at BNL would do the design and fabrication in house.

3.1.4 EBIS vacuum system

3.1.4.1 Vacuum requirements for the ionization region

Ion confinement times as long as 100 ms may have to be used to reach the charge states of interest. The background pressure in the trap region should be low enough that one does not produce a significant number of ions from the background gas. For a residual gas pressure $P=1 \times 10^{-10}$ Torr, one estimates that less than 2% of accumulated ions in a trap will be background gas ions. One can tolerate values even a factor of 10 above this, so this gives a range of acceptable vacuum conditions in EBIS ($10^{-9} - 10^{-10}$ Torr) and determines requirements to the vacuum technology. Requirements for the concentration of hydrogen are less rigorous, and its partial pressure can be 5 times higher.

Since background gas ions are typically lighter than injected ions, their presence may result in a beneficial cooling of the injected ions. However, it is advantageous to be able to inject cooling ions into the electron beam in a controlled way, so the above estimate for the vacuum is still desirable. Requirements on the pressure of residual gas in the electron gun region are dictated primarily by the need for proper conditions for operation of cathode, and in the electron collector by the need for stable transmission of the electron beam without plasma formation. Normally, the pressure in the regions of electron gun and electron collector can be higher than in the ionization region, provided there is efficient vacuum separation between the sections.

3.1.4.2 Requirements to the vacuum system

Based on our experience with the EBTS the requirements to the vacuum system are:

- All parts with surfaces exposed to the central chamber should be vacuum fired (baked in a vacuum oven to 900⁰ C for 2 hours) before installation in EBIS. This requires use of steel 316LE for ConFlat flanges.
- Materials of all other parts should allow baking to 3000C.
- Regions with high outgassing rate (electron collector, electron gun) should be separated as much as possible from the central chamber containing the ion trap. Practically, the area of direct connection between the central chamber and adjacent electron gun and electron collector chambers should be approximately 50% larger than the cross-sectional area of the electron beam in the regions of separation. This means that the conductivity between the central and adjacent chambers should be ~100 l/s.
- To have a better vacuum and faster turnaround times the pumping speed in the central chamber should be ~10 times higher than it is presently in EBTS, i.e. about 20,000 l/s. For the same reason the central region containing the ion trap should be preserved from venting to atmosphere during maintenance or upgrade operations with electron gun and electron collector by separating it from these regions with gate valves.

3.1.4.3 Structure of the RHIC EBIS vacuum system

Our experience in the operation of EBTS has proven that high vacuum in the ionization region of the EBIS can be achieved without having the drift structure at cryogenic temperatures, by using conventional vacuum technology and pumps. Still, the vacuum system of the RHIC EBIS will include some improvements to reduce further the flow of residual gas to the ion trap and improve the pumping of gas created in the central chamber. These modifications include:

- Increase vacuum conductivity between the middle part of the central chamber and the side parts of this chamber where pumps are located, by increasing the diameter of the central chamber from 4” (as it is now in EBTS) to 6”. It follows that a larger diameter of the bore of the solenoid is required.
- Reduce the turnaround time for the vacuum system by using thermo resistant materials on the exterior of vacuum chambers, so there will be no need to remove sensitive elements prior to bakeout. One should make a permanent system of electrical heaters and temperature sensors connected to a bakeout station.
- Introduce an additional stage of vacuum separation between electron collector and the central vacuum chamber, which should reduce the flux of residual gas from the heavily outgassing electron collector into the central region by another factor of 10.
- Increase the pumping speed in the central chamber by using non-evaporable getters (NEG) in the region of the ion trap.
- Separate the electron gun and electron collector from the central vacuum chamber with two gate valves.

The proposed structure of the vacuum system of the RHIC EBIS is presented in Fig.3.1.4.3.1.

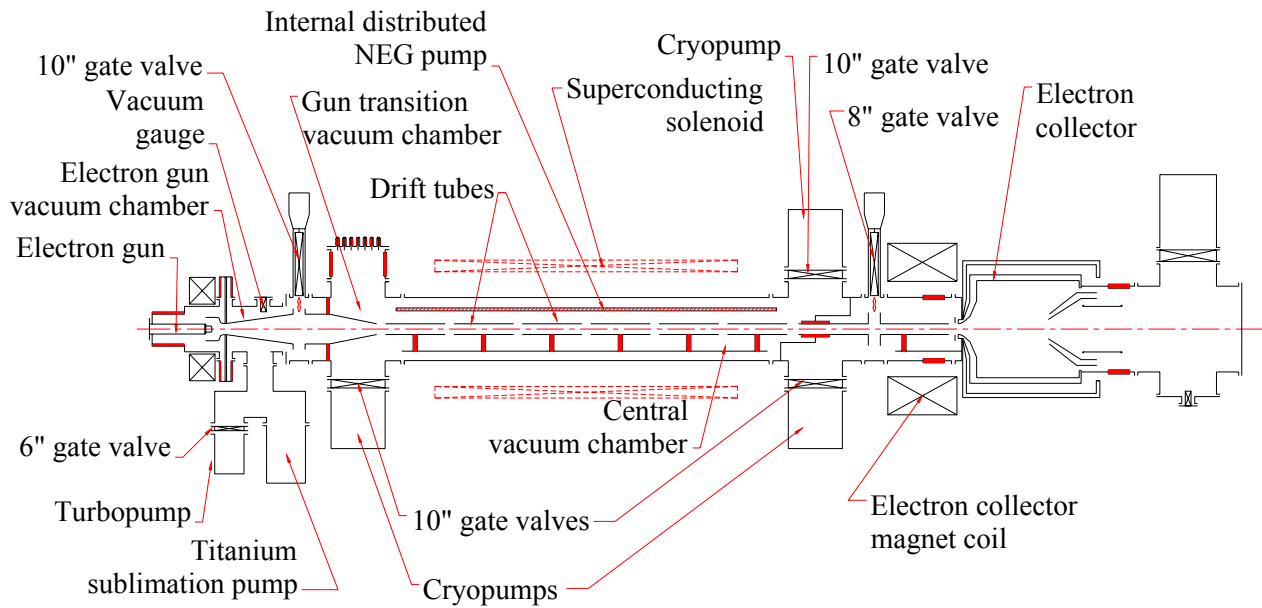


Fig. 3.1.4.3.1 Vacuum system of RHIC EBIS

3.1.5 Seeding the EBIS trap

The primary means of seeding the trap of the RHIC EBIS will be injection and trapping of singly charged ions from an external ion source. This technique has been used very successfully on other EBISs, as well as on EBTS, and allows one to produce a very narrow charge state distribution. The requirements of the external source are relatively modest, needing to produce currents of only about $100 \mu\text{A}$. The commercially available Chordis source has been used successfully on the Stockholm EBIS to produce a wide range of beams from both solids and gasses. If one needs to switch quickly (pulse-to-pulse) between two species, two external injection sources could be used. The transport line from the external source to the EBIS will provide magnetic mass analysis of injected ions.

3.1.6 EBIS Power Supply Requirements

For injection into the RFQ, ions must be accelerated from +50 kV to ground potential. At least part of this energy comes from the biasing of the trap region relative to the rest of source. The remainder of the energy must come from a biasing of the entire source with respect to ground. Applying all voltages internally would be more convenient, but it leads to more difficult design issues due to the presence of high voltages in a strong magnetic field. Therefore, we will incorporate both internal and external biasing in the design. The mode of operation can be summarized as follows: With the EBIS platform at ground potential, the primary ions are injected into the EBIS at 10-20kV energy from an auxiliary ion source. The ion energy for capture by the EBIS can be adjusted by using both the EBIS drift tube supplies and the auxiliary ion source bias supply. The ions are then confined within the EBIS and multiplied to the proper charge state during a period of approximately 30ms. Before the highly charged ions are expelled from the trap for transport to the RFQ, the EBIS platform voltage is pulsed on such that the extracted ion energy is ~50kV. The various voltage platforms are described below, and are shown schematically in Fig. 3.1.6.1.

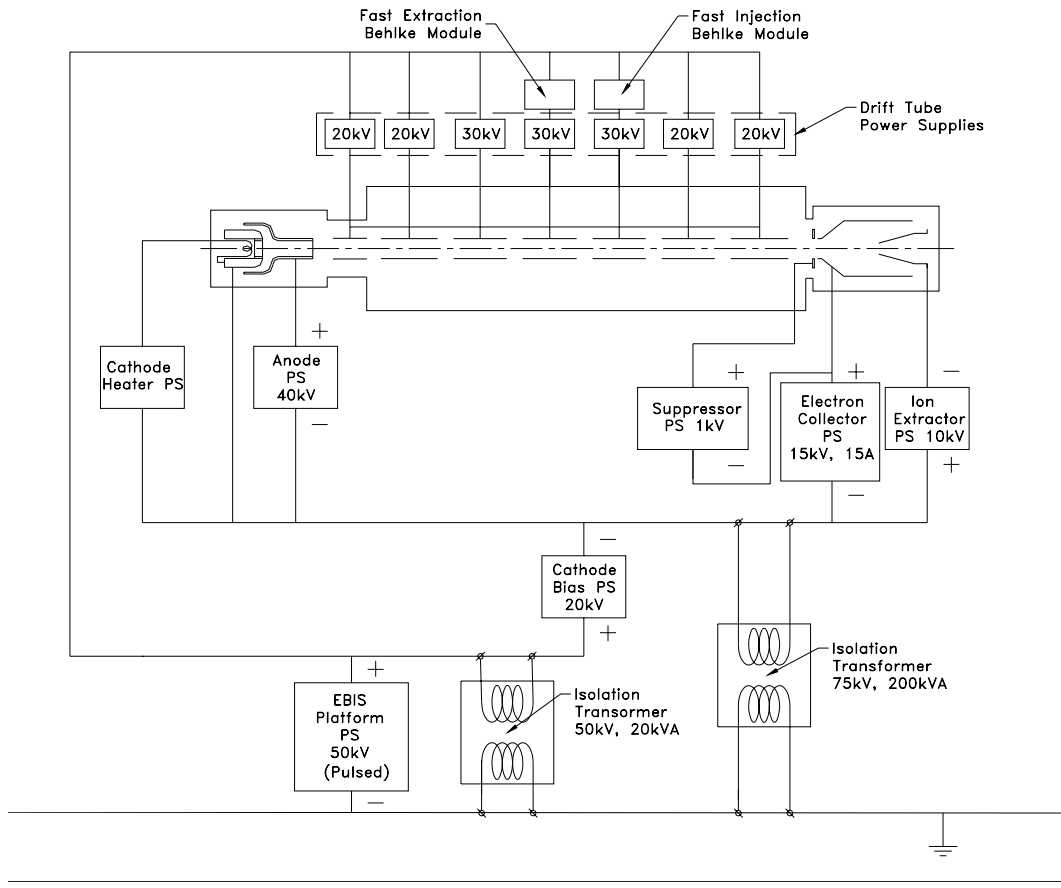


Fig. 3.1.6.1 Schematic of the EBIS voltage platforms

Laboratory platform (ground):

This platform contains the operator interface for the EBIS controls and diagnostics. The extraction beamline will also be referenced to laboratory ground where applicable. The power supply to bias the EBIS platform to attain the full extracted ion energy and the the supply to bias the auxiliary ion source for seeding the EBIS via external ion injection will be reference to the Laboratory platform.

- EBIS platform bias supply
- Auxiliary ion source bias supply
- Mass analyzer supply (for auxiliary ion source)
- External beamline optics power supplies

EBIS source platform:

With this platform the EBIS, including the vacuum chamber and solenoid, will be elevated briefly to approximately +30 kV for extraction and transport of highly charged ions to the RFQ. The remaining 20 kV necessary to achieve the 50 kV RFQ injection energy would then be provided by biasing internal electrodes. Active bipolar supplies allow short pulse high energy extraction. In order to produce very fast ($\sim 10\mu\text{s}$) extracted ion pulses, custom built supplies based on 20 kV Behlke switches would reside on this platform; fast extraction has already been demonstrated on our EBTS using a prototype Behlke-based supply. Power supplies will be controlled by the EBIS voltage controller via digital and analog optical links. During the ion injection and confinement periods, the EBIS source is nominally at laboratory ground potential. The source support will be constructed to hold off up to 50 kV. Power supplies on this platform are:

- Cathode bias supply (biases electron gun platform)
- Drift tube power supplies
- Behlke fast injection and extraction modules
- Gun, main, and collector solenoid power supplies
- Correction solenoids and transverse magnetic steering coil supplies.

Electron gun (cathode) platform:

This is an internal platform that contains the main electrodes responsible for establishing and collecting the electron beam. The power required for collecting the electron beam is provided directly to this platform by a 200 KVA (nominal) isolation transformer. Power supplies belonging to this platform are:

- Cathode heater
- Anode
- Electron collector (and suppressor)
- Ion extractor

In this concept, a low current acceleration supply ($\sim 10\text{mA}$) is used to establish electron beam propagation in the trap region, while a high current collector supply ($\sim 15\text{A}$, 15kV) is used to collect the electron beam. The accelerator provides stable electron beam launch conditions, and protects against excessive electron beam loss since the capability of the power supply to provide current is low. In this configuration, it should be possible to relax the voltage stability requirement for the high power electron collector supply. The ion injection and extraction will be synchronized with

the line frequency, since the collector voltage is still an element influencing the optics of the extracted ion beam.

Auxiliary ion source platform:

This platform contains the ion source used to seed the EBIS with primary low charged ions of the selected species. The platform will be operated up to +30 kV and will contain supplies relevant to the specific type source, such as:

- Heater
- Arc pulser
- Extractor
- Lens
- Deflector

3.1.7 EBIS Controls and Timing

The EBIS system consists of power supplies for magnets, electrostatic lenses and drift tubes. Primary control for EBIS consists of timing and waveform generation for the power supplies. Waveform generation will be accomplished mainly with the use of digital-to-analog converters (D/A). Primary data acquisition for EBIS will be voltage and/or current read backs from the high voltage power supplies and read backs from beam instrumentation devices. The EBIS system will have approximately 100 signals that will need to be acquired. Out of these 100 signals, 20 will be fast pulsing signals (approximately 10 μ s). Data acquisition will be accomplished mainly with the use of analog-to-digital converters (A/D). Secondary data acquisition needs for EBIS are temperature and pressure sensor readbacks.

The EBIS voltage controller issues all internal timing signals relevant to ion source operation. In particular, it controls EBIS trap electrode timing and voltage references, auxiliary ion source timing and switching of optics in the beam lines of the EBIS subsystem. Analog and digital signals are sent to power supplies and timing devices over optical links where necessary. The analog optical links for the fast power supplies must be good to about 20 μ s. This allows monitoring by an oscilloscope at the ground platform. Timing will also be an important input to an EBIS data acquisition system since data must be taken from the EBIS system at precise times.

3.2 LEBT

The Low Energy Beam Transport (LEBT) transports the beam from the EBIS and matches it to the RFQ. The layout was shown in Fig. 3.1. The LEBT is 1.4 meters long and consists of two solenoid magnets for transverse matching, two sets of transverse steerers, and a Y-chamber in the middle of the line. One arm of this chamber allows ions from an external ion source to be injected into the EBIS trap. In the second arm extracted ions can be deflected into a time-of-flight diagnostic.

The beam from the EBIS source has to be matched into the RFQ, which needs a small, highly convergent beam. The beam out of EBIS is symmetric in x and y, as is the RFQ acceptance, so one needs control of only two degrees of freedom for matching. Table 3.2.1 shows the Twiss parameters at the beginning and end of the LEBT. Figure 3.2.1 shows the beam envelopes along the LEBT (output from TRACE code). The magnetic fields required for the two transverse matching solenoids are 4 and 7.5 kG. There is about 1 meter between these two solenoids for the ion injection and diagnostics.

Table 3.2.1: Twiss parameters at beginning and end of the LEBT.

Parameters	Beginning of LEBT	End of LEBT	Units
Alpha_x	-5.180	2.630	
Beta_x	9.136	0.1076	mm/mrad
Emittance (4*rms,unnorm)	85.17	85.17	π mm mrad
Alpha_y	-5.180	2.630	
Beta_y	9.136	0.1076	mm/mrad
Emittance(4*rms, unnorm)	85.17	85.17	π mm mrad

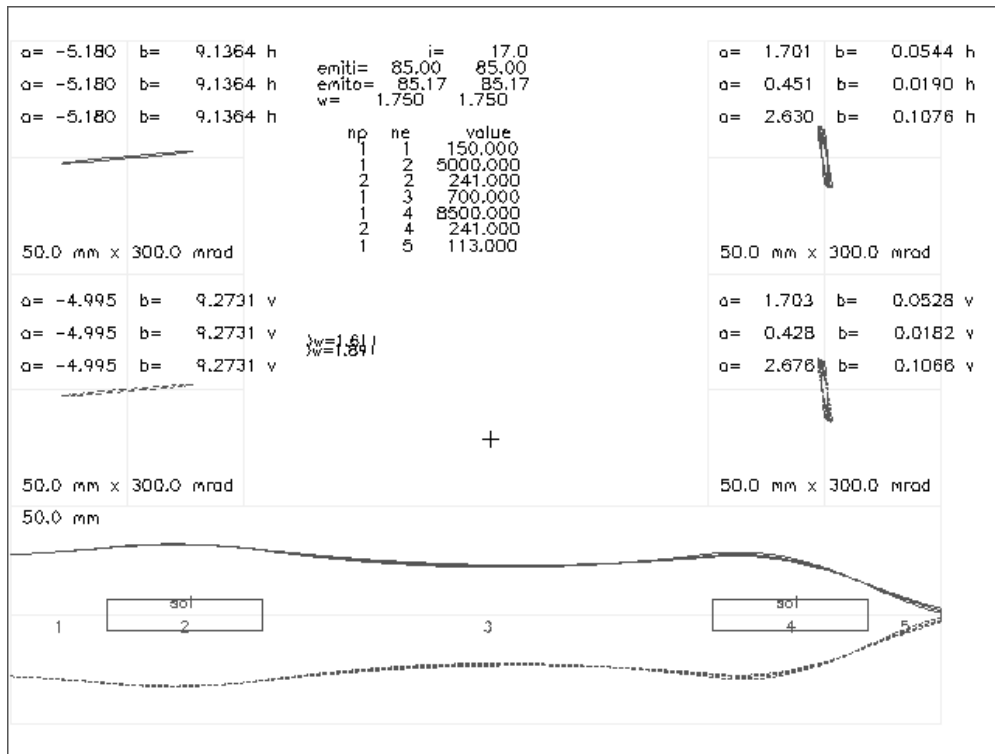


Fig. 3.2.1 TRACE output showing beam transport from EBIS to RFQ

These calculations have been done including the effects of the space charge at the full beam current of 8.5 mA (all charge states), since the pulse length is too short for neutralization to occur. If the charge-state distribution were broader, as in an ECR or LIS, the space charge from a much higher total beam current would present problems in matching.

Calculations have also been done where the beam is matched into the RFQ with electrostatic lenses, and this is still a viable option that is being considered.

3.3 RFQ

3.3.1 Choice of Parameters

The EBIS output energy is 8.5 keV/amu. The RFQ output energy is 300 keV/amu, which is a comfortable input energy for the IH structure. The frequency chosen is 101.28 MHz. The focusing force in the RFQ is proportional to $1/(\text{rf wave length})^2$, and this frequency provides a good focusing for a relatively low q/m beam. Another consideration has been the fact that there are several existing RFQs operating at this frequency. The emittance from the EBIS source has not yet been fully determined, but based on the available data we estimate it to be about 0.35π mm mrad (normalized, 90%). The acceptance of the RFQ in the present design is comfortable, at 1.7π mm mrad (norm.), with an aperture radius of 6 mm.

3.3.2 Specifications

At a frequency of 101.28 MHz, a four rod RFQ can be easily designed and built, and would be very similar to the CERN heavy ion RFQ. Table 3.3.2.1 shows some parameters and specifications of the two RFQs. Figure 3.3.2.1, shows the beam optics relevant parameters along the length of the RFQ.

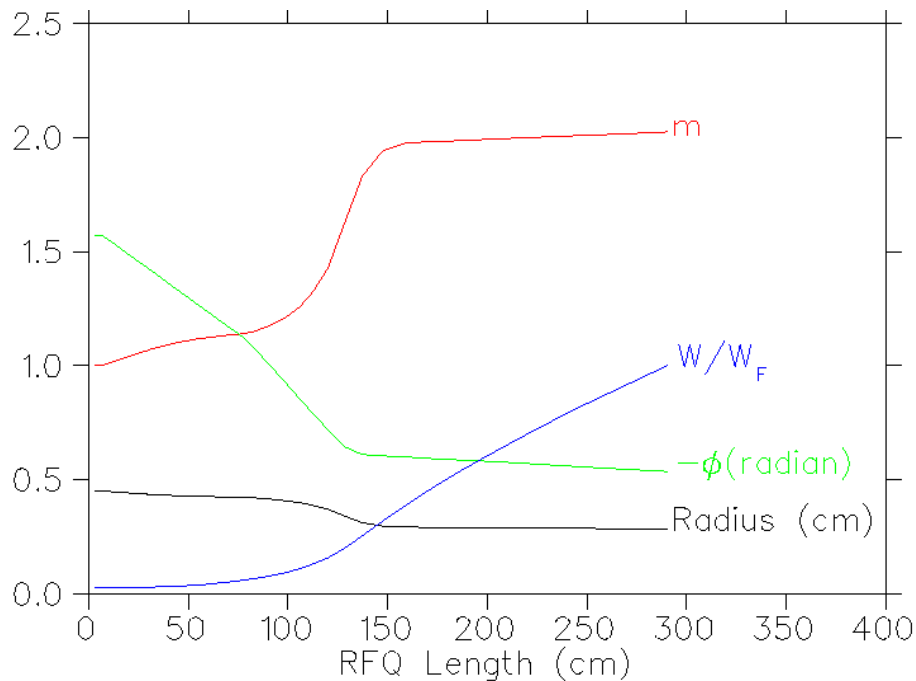


Figure 3.3.2.1 Optics design parameters for the RFQ

Table 3.3.2.1: Specifications for the RFQ

Parameters	BNL	CERN	Units
Type	4-rod	4-rod	
Q/m	0.16-0.5	0.12	
Input Energy	8.5	2.5	keV/amu
Output Energy	300	250	keV/amu
Frequency	101.28	101.28	MHz
Max rep rate	10	10	Hz
Length	2.96	2.5	meters
Number of cells	236		
Aperture Radius	0.006	.0045	meters
Voltage	92	70	kV
E(surface)	20.8	≤ 23	MV/m
RF Power	< 350	< 350	kW
Acceptance	1.7	> 0.8	pi mm mrad (nor)
Input Emittance	0.35		pi mm mrad, nor, 90%
Output Emittance (trans)	0.375		pi mm mrad, nor, 90%
Output Emittance (longit)	0.75		pi MeV deg
Transmission	97	93	%
Bravery factor	1.8	≤ 2	Kilpatrick

3.3.3 Beam Dynamics

To keep the length short, the RFQ is designed using a modified LANL recipe [3-1]. The RFQ has four sections, (1) radial matching section, (2) shaper (3) buncher and (4) accelerating section. The design of the first three sections follows the same recipe as LANL's [3-2], but in the acceleration section, at first the current limit is kept constant while the modulation factor m grows by 2, after which m is kept constant. This reduces the RFQ length, which is only 3 meters. Figure 3.3.3.1 shows the current limits along the RFQ and Fig. 3.3.3.2 shows the various beam profiles along the RFQ. Simulations show that the beam losses are concentrated in the RFQ during the bunching process. Fig. 3.3.3.3 shows the transmission as a function of input emittance. There is essentially no calculated emittance growth. Fig. 3.3.3.4 shows the transmission as the input energy is varied. This shows that the RFQ transmission will remain good even if the EBIS beam energy spread is increased (i.e. voltage in the EBIS trap is ramped to decrease ion pulse width). The RFQ transmission remains $> 80\%$ even for currents in excess of 35 mA. Simulations also show that transmission is high for charge states neighboring the desired charge state, that is, the RFQ will not act as a good filter for the off-charge states.

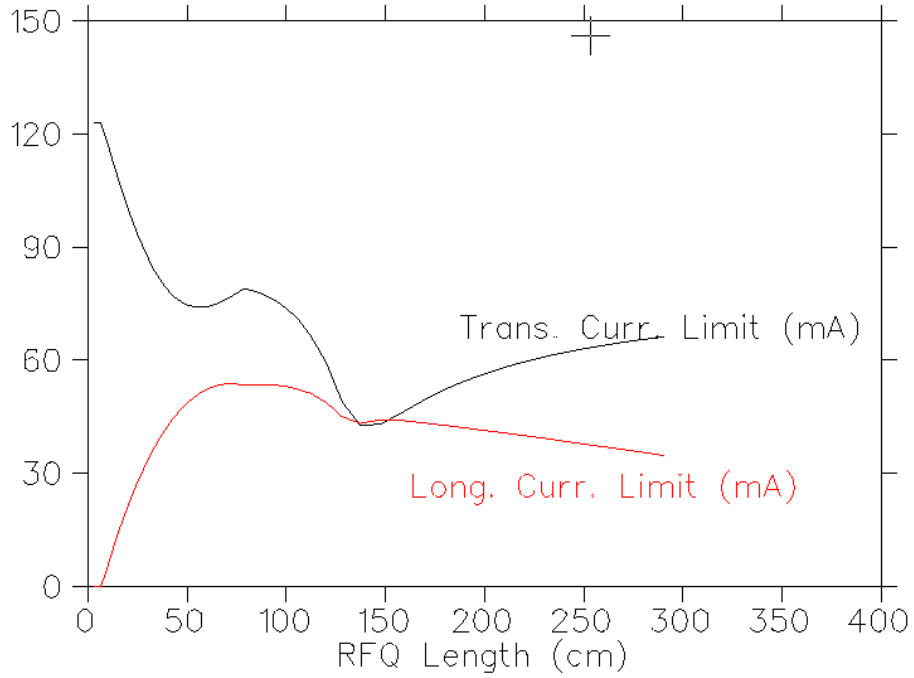


Fig. 3.3.3.1 Current limits along the RFQ

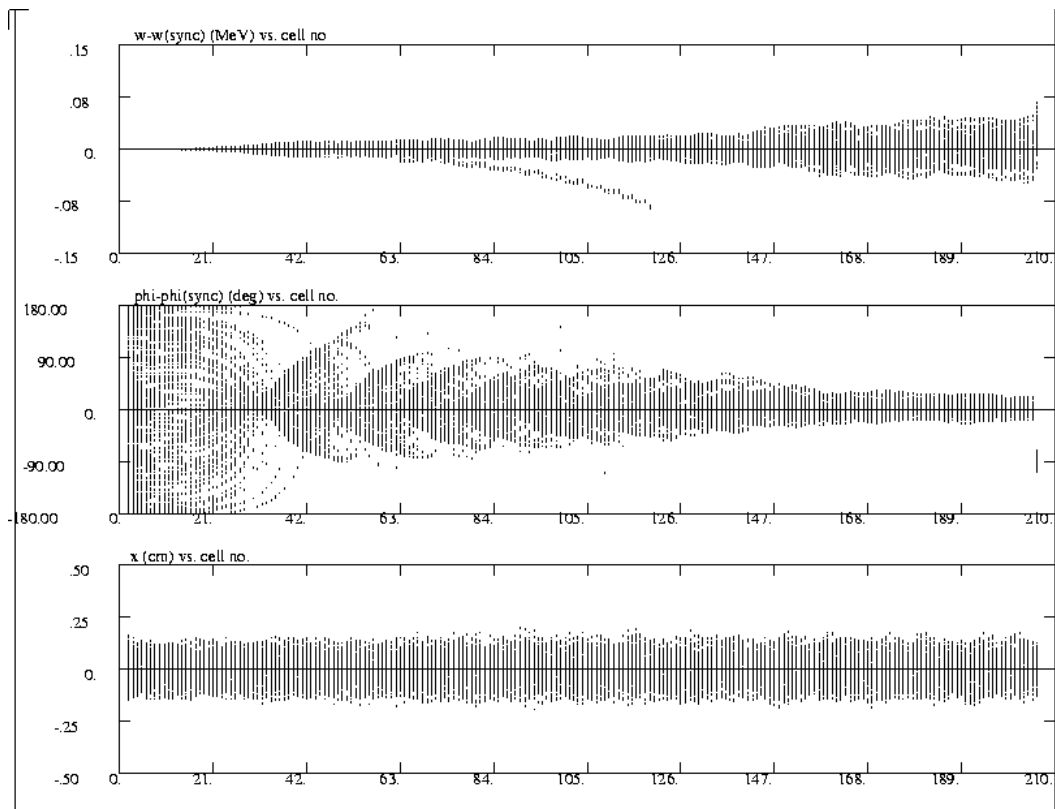


Fig. 3.3.3.2 Variation of energy spread, phase spread, and x-profile along the RFQ

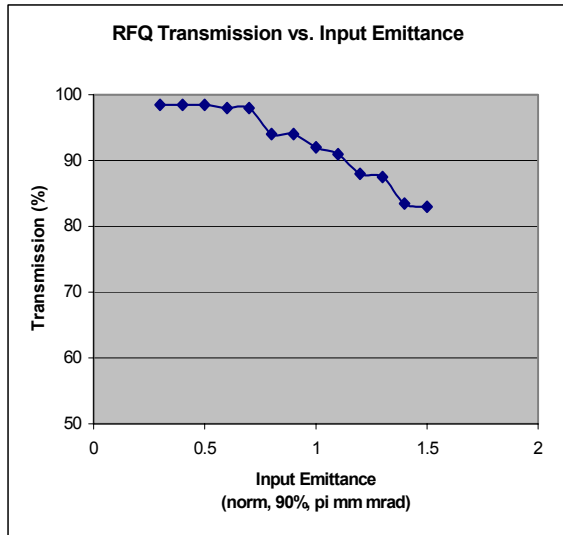


Fig. 3.3.3.3 RFQ transmission vs. input emittance.

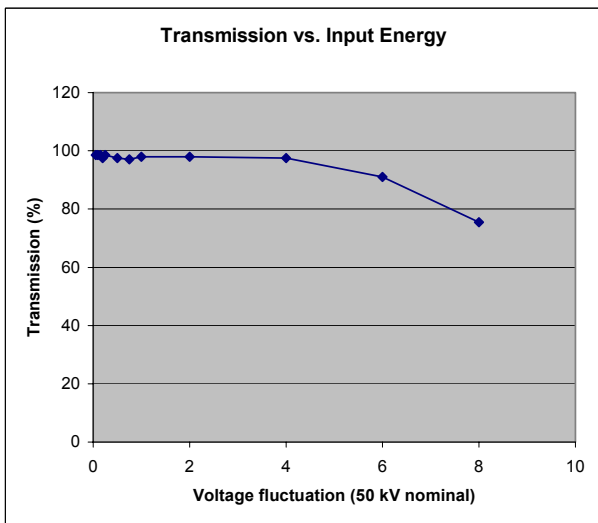


Fig. 3.3.3.4 RFQ transmission vs. input energy change.

3.4 MEBT

The purpose of the Medium Energy Beam Transport (MEBT) is to match the beam from the RFQ to the IH structure in all three planes (two transverse, and longitudinal). The RFQ has a FODO lattice with $1 \beta\lambda$ period and IH structure has solenoidal focusing which is symmetric in x and y. The RFQ and the IH structure have the same RF frequency of 101.28 MHz. Table 3.4.1 shows the Twiss parameters at output of the RFQ and input of the IH structure.

Table 3.4.1: Twiss parameters at the end of the RFQ and entrance of the IH structure.

Parameter	End of RFQ	Entrance of IH	units
Alpha_x	1.34	0.94	
Beta_x	0.163	0.416	mm/mrad
Emittance (5*rms,unnorm)	21.72	21.72	pi mm mrad
Alpha_y	-1.06	0.703	
Beta_y	0.134	0.644	mm/mrad
Emittance(5*rms, unnorm)	21.72	21.72	pi mm mrad
Alpha_z	0.6800	-0.0534	
Beta_z	0.0152	0.0033	deg/keV
Emittance (5*rms)	32543	32543	pi keV deg

The MEBT requires 6 controllable elements to match the beam in all three planes, four in the transverse plane and two in the longitudinal plane. Because the RFQ is a strong focusing structure, the beam from the RFQ is highly divergent in one transverse plane and highly convergent in the other transverse plane. After passing the RFQ high energy endflange, gate valve, and a current transformer, the beam has usually become divergent in the both planes by the time it reaches the first quadrupole. To avoid this problem we are using a small permanent magnet quadrupole placed in the high-energy end flange of the RFQ. (This technique has been employed in our proton RFQ). There are four more quadrupoles to provide four degrees of freedom in the transverse plane. In the longitudinal plane we use one buncher and the position of the buncher to match the beam to the IH structure. Thus we have 5 active controls to match beam instead of six. Figure 3.4.1 shows the TRACE3D output for the MEBT. There is enough space in the MEBT to accommodate the diagnostics.

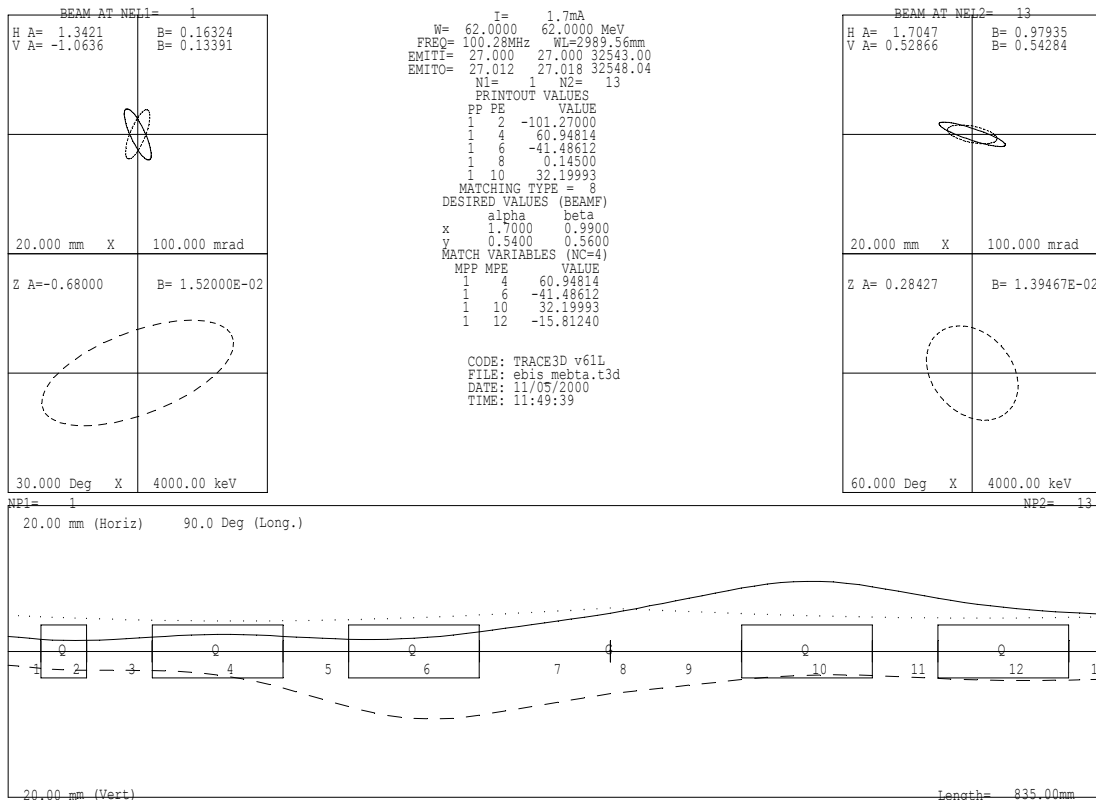


Fig. 3.4.1 TRACE3D output showing the MEBT optics

3.5 IH Linac

For the baseline design, we have chosen an Interdigital-H (IH) structure, as been used at CERN for the Pb linac, and at GSI. This will be a single-cavity, designed for a fixed output velocity, independent of the q/m of the desired beam (cavity gradient is adjusted for different q/m 's, to maintain a fixed velocity profile). In the first year of the project, we will continue to investigate alternative structures, including independently phased superconducting cavities, similar to the ATLAS structure at Argonne, or the room temperature structure used for the TRIUMF rare-ion accelerator. Either of these would offer the potential advantage of allowing acceleration to higher energies for higher q/m ions.

3.5.1 Specification of parameters

As mentioned previously, we have selected a minimal final energy of 2 MeV/amu into the AGS booster, to reduce the space charge tune shift and the electron capture cross section at injection. The linac frequency is chosen to be 101.28 MHz, which is in the same as the CERN Pb IH linac. This design is an extension of CERN Pb linac in which the beam dynamics concept of "combined zero degree synchronous particle sections" is used.

The linac has one tank, 4 meters long, with two quadrupole triplets inside for focusing. The maximum field on the axis will be 13.5 MV/m. The gap voltage distribution is adjusted by changing the capacity distribution between the adjacent drift tubes to match the velocity profile. Table 3.5.1.1 shows the main parameters of the IH linac.

Table 3.5.1.1: Main parameters of the IH linac

Parameters	BNL	CERN Tank 1	Units
Q/m	0.16-0.5	0.12	
Input energy	0.300	0.250	MeV/amu
Output Energy	2.0	1.87	MeV/amu
Frequency	101.28	101.28	MHz
Max rep rate	10	10	Hz
Length	4.0	3.57	Meters
Input emittance	0.55		pi mm mrad, norm, 90%
Output emittance	0.61		pi mm mrad, norm, 90%
Output energy spread	20.0		keV/amu
Transmission	100		%

3.5.2 Beam Dynamics

We have used the computer code LORAS [3-3] to design and simulate the IH linac. Figure 3.5.2.1 shows the beam profiles (x, and y) along the linac. figure 3.5.2.2 shows the phase width and energy width profiles along the linac. Figure 3.5.2.3-5 show the input and output phase space projections in the x, y, and phase-energy planes, respectively.

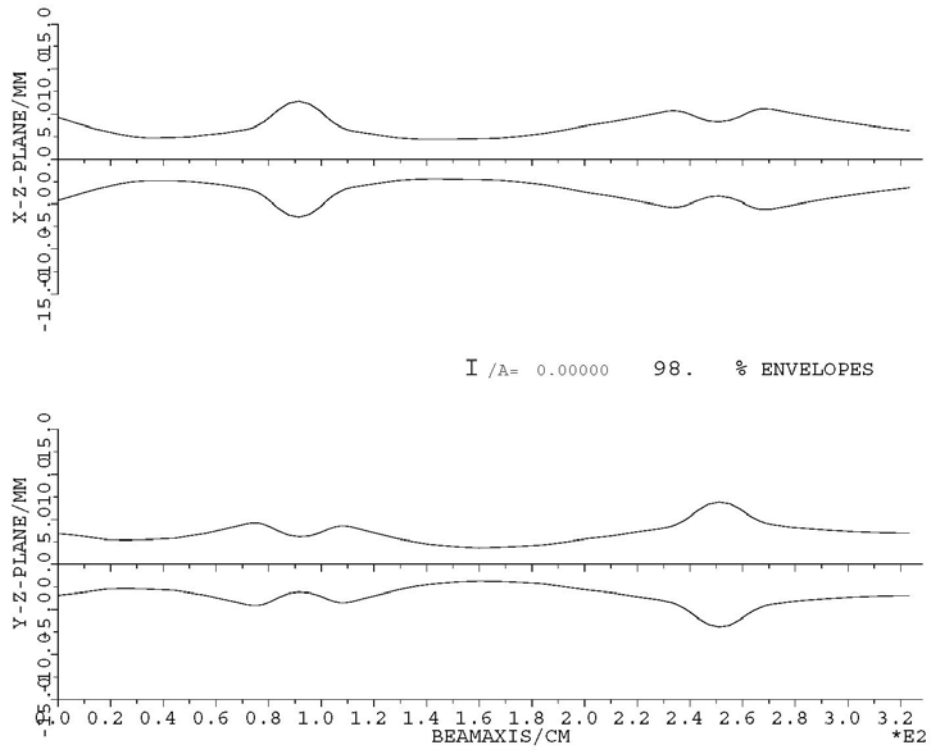


Fig. 3.5.2.1 x and y beam profiles along the linac

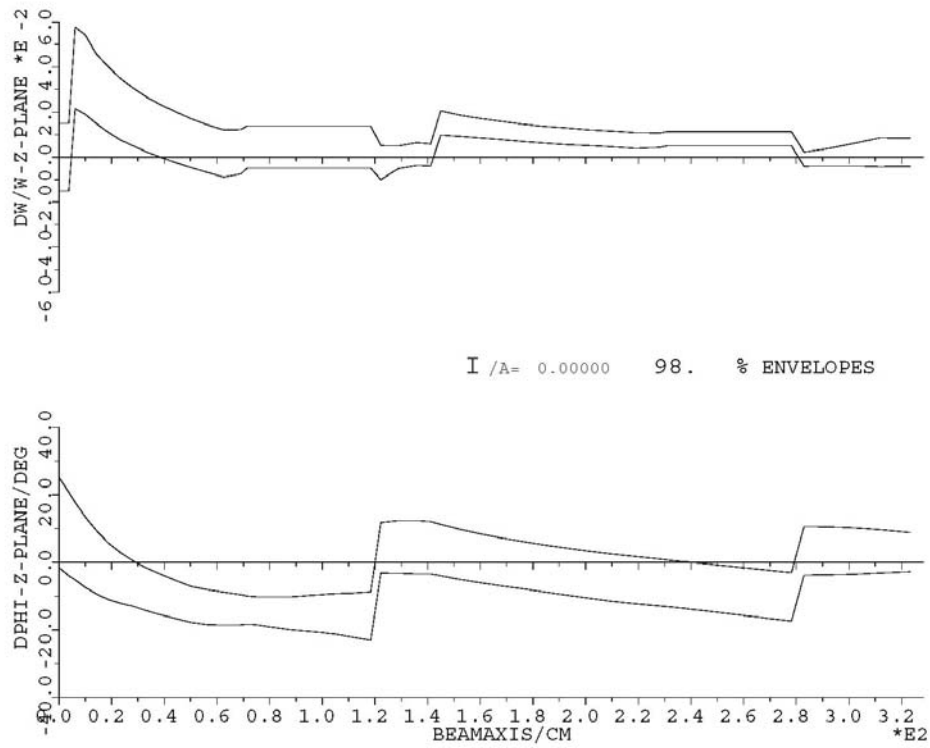


Fig. 3.5.2.2 Phase width and energy width along the linac

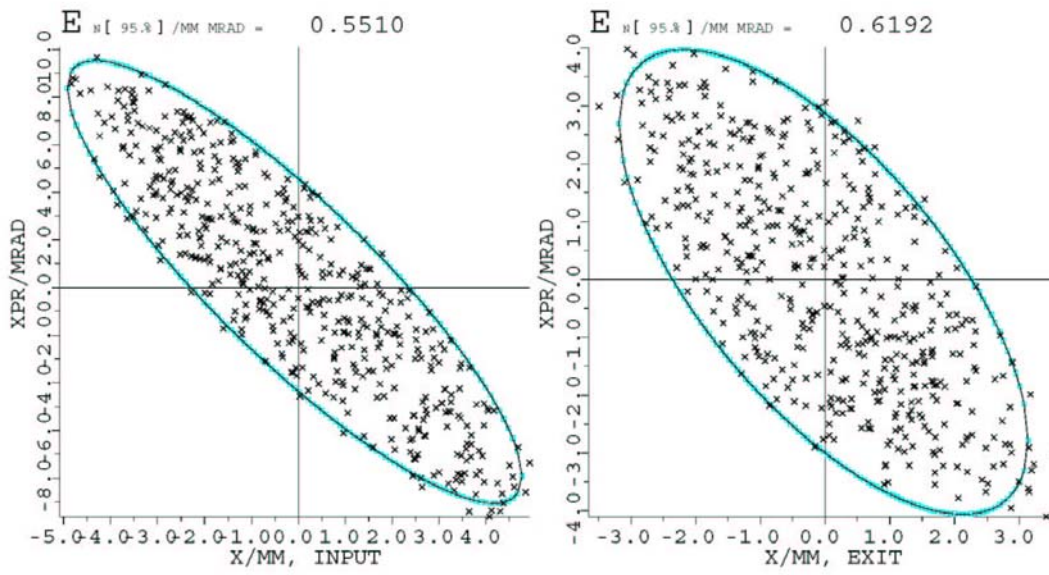


Fig 3.5.2.3 Input and output x-phase space

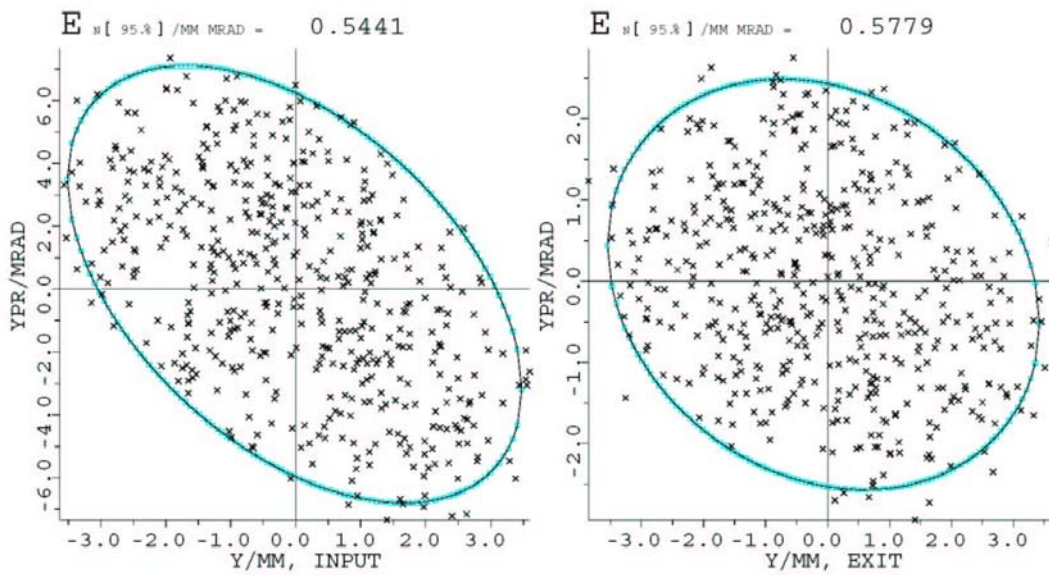


Fig. 3.5.2.4 Input and output y-phase space

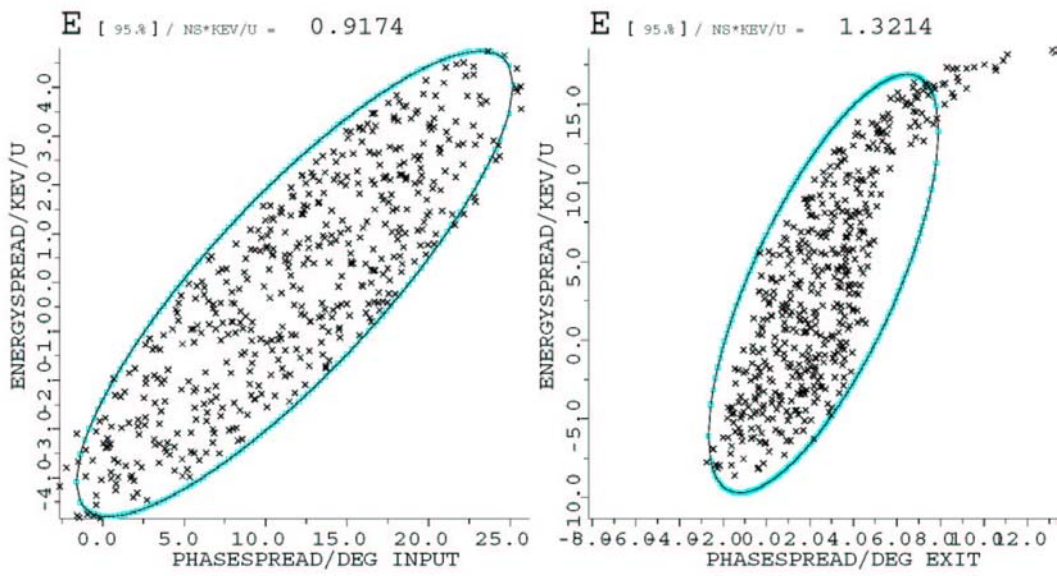


Fig. 3.5.2.5 Input and output longitudinal phase space

3.6 HEBT

The High Energy Beam Transport (HEBT) matches beam transversely from the linac to Booster injection, minimizes the energy spread at the injection, provides ion charge state discrimination, and provides space for diagnostics. The preinjector is located in the lower equipment bay of the 200 MeV H^- linac. In order to provide the necessary space for power supplies and water cooling, a 2-story extension will be added onto the building, providing an additional 2800 ft² of floor space. A beamline penetration through the linac shielding provides a short, direct path into the Booster allowing injection using the existing heavy ion inflector. The line is shown schematically in Figure 3.6.1. Since the RFQ and linac will not eliminate all unwanted charge states, the line will be designed for charge discrimination. A debuncher cavity will be used in HEBT to rotate the longitudinal phase space to minimize the energy spread at Booster injection. Table 3.6.1 gives the Twiss parameters at the end of the linac and entrance of the booster.

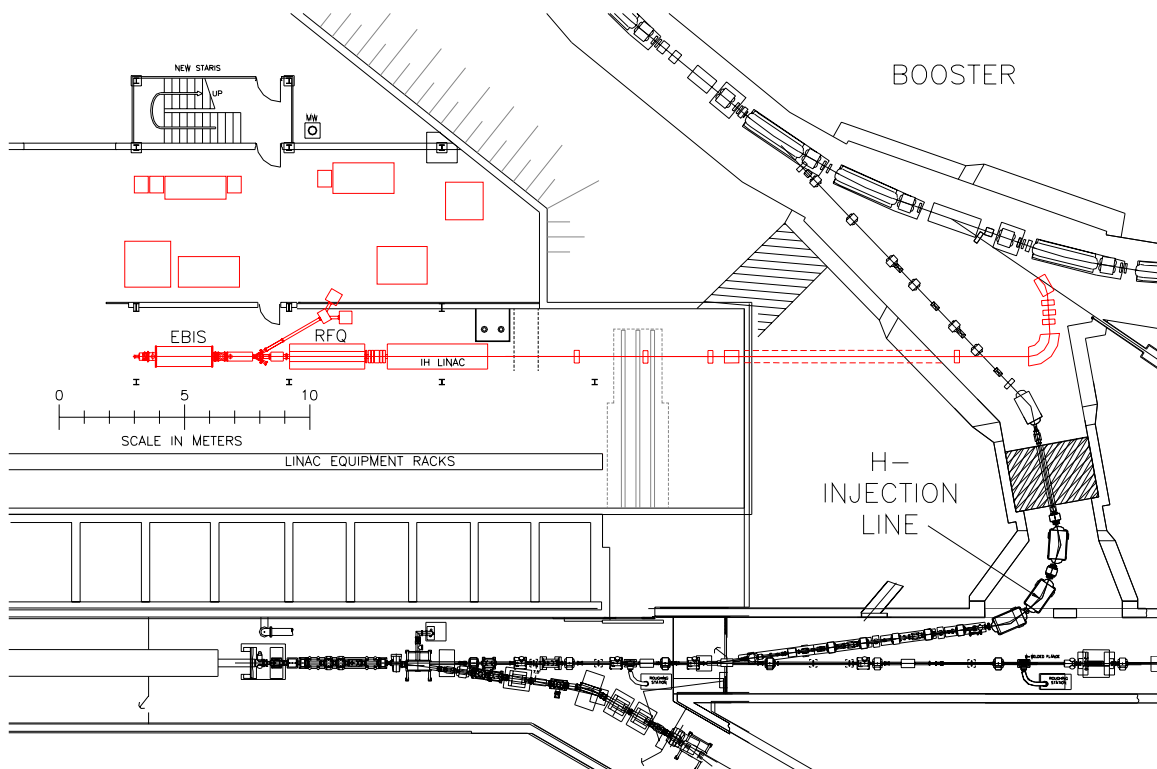


Figure 3.6.1 Schematic showing the preinjector in the lower equipment bay of the 200 MeV Linac.

Table 3.6.1: Twiss parameters at end of IH Linac entrance of the Booster

Parameters	End of IH Linac	Entrance to Booster	Units
Alpha _x	1.2000	-1.7277	
Beta _x	2.1736	11.008	mm/mrad
Emittance (5*rms, unnorm)	9.2	9.21	pi mm mrad
Alpha _y	0.28.00	0.82163	
Beta _y	1.4397	4.8321	mm/mrad
Emittance (5*rms, unnorm)	9.2	9.2	pi mmrad
Energy spread (for 5 rms emittance)	+180	+170	keV

3.7 Diagnostics and Controls

The type and location of the new diagnostics required for the preinjector are listed below. Following the merging with the existing TTB line, existing diagnostics are used, with the exception of two new beam transformers and one new Faraday cup.

- Current Transformers (7)
EBIS output, RFQ input, RFQ output, IH input, IH output, 2 in HEBT
- Emittance (2)
1 between EBIS and RFQ, 1 between RFQ and IH
- Multiwire/Faraday cup combination (3)
3 in HEBT
- Fast Faraday cup (1)
1 after debuncher (use existing unit from proton linac)

Controls will be implemented in the same way as other recent installations such as the new polarized ion source and Booster Application Facility. The existing AGS/RHIC controls Ethernet will be extended to the new building. Standard AGS/RHIC Front-End chassis with processors and utility modules will be provided for controls interfacing. Workstations and X-terminals will be placed at several key equipment locations. All transport line diagnostics are similar to existing equipment, and applications are already existing. Vacuum equipment will be controlled via PLC's, with a PLC interface module to tie in to the control system.

3.8 RF Systems

Five rf systems will be required. The RFQ and Linac will each require a 1ms pulse width, 10 Hz, 350 kW peak power tetrode unit, similar to a CERN system. The three bunchers will each use 4kW solid state amplifier. All systems will use amplitude and phase regulation, and frequency tuning.

3.9 Vacuum systems

The EBIS vacuum system was described in a previous section. The RFQ and IH linac will each have two cryopumps, similar to our existing proton RFQ. All metal gaskets (Conflat) will be used in the transport lines. The LEBT and MEBT sections will be unbaked. For convenience in operation and maintenance, sector gate valves are included as shown in the schematic of the vacuum system, Fig. 3.9.1. The HEBT line will be a baked system. Non-evaporative getter (NEG) strips inside the beam pipe will be used, along with ion pumps, exactly as used in the Tandem-to- Booster transport line. A fast closing valve will be installed in HEBT just before the junction with TTB. Vacuum interlocking, and valve and pump control will be via a PLC-based system.

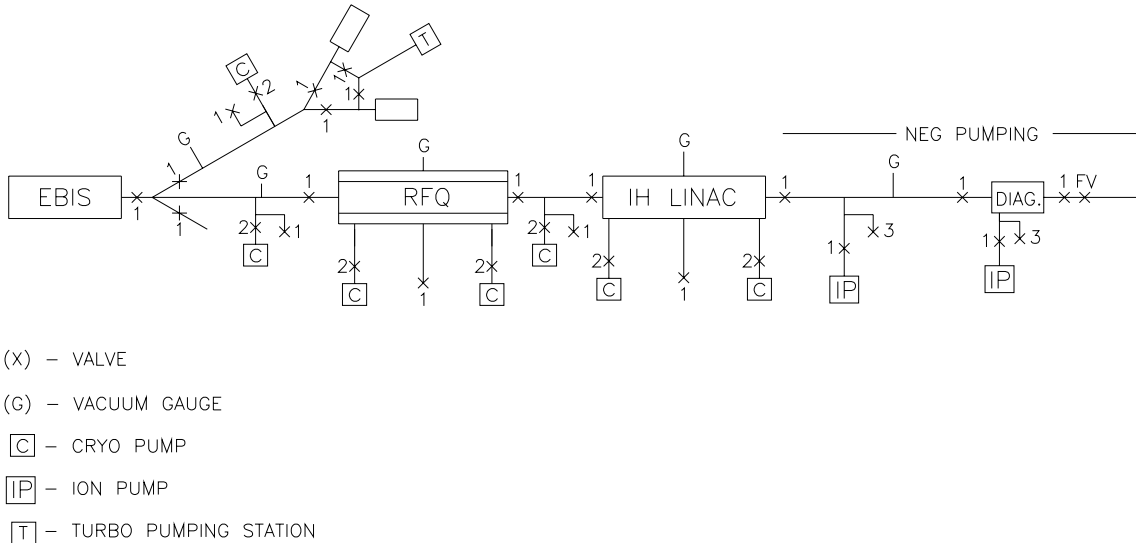


Fig. 3.9.1 Schematic of the vacuum system

3.10 RFQ & linac water system

According to the design specifications, the combined Linac and RFQ need a minimum of 7 kW of cooling. The cooling water has to be maintained in a ± 1 C range to keep the RF system on resonance. The design of the cooling system is based on the systems used for cooling the cavities in the 200 MeV linac. A 120 GPM flow rate is specified for good convective transfer to reduce time delay in reaching equilibrium. The basic system consists of two 10 hp pumps (one is backup), an appropriately sized heat exchanger, a three-way mixing valve, and temperature control system.

4 Booster Injection with the EBIS Beam

4.1 EBIS Beam

The expected parameters of the EBIS beam at the Booster are presented in Table 4.1.1.

Table 4.1.1 Expected beam parameters at Booster injection

Au^{32+}			Unit
Particles per pulse	N	3	10^9
Kinetic energy	E_k	2	MeV / u
	β	0.0652	
	γ	1.002	
Pulse width	d	10 - 40	μs
Energy spread	ΔE	± 2	keV / u
Momentum spread	$\Delta \rho / \rho$	± 0.05	%
Norm. 95% emittance	$\varepsilon_{N,95}$	0.7	$\pi \mu m$

The pulse width will allow for 1 to 4 turn injection at the Booster. It may also be possible to extract ions from the source in short bursts to match directly the Booster rf buckets. With the Booster RF harmonic number 4 or 6, this would require a bunch length about 1.23 μs or 0.83 μs , respectively. The energy spread and the transverse emittance should be unchanged with this ‘‘bunched’’ beam.

The beam energy spread at the exit of the Linac is $\pm 2 keV / u$, which is reduced by a debuncher to $\pm 2 keV / u$. This is crucial for keeping the Booster beam longitudinal emittance small. The transverse profile of the beam will be Gaussian-like.

4.2 Space Charge Effect

The space charge effect is estimated by the incoherent tune spread

$$\Delta \nu_{inc} = \frac{-3NQr_0}{2\pi AB_f \beta \gamma^2 \varepsilon_{N,95}} \quad (1)$$

where Q and A are the charge state and atomic mass, respectively, r_0 is the classical radius of proton, and B_f is the bunching factor. The bunching factor at early acceleration is considered to be ≤ 0.4 .

With 1 to 4 turn injection, the calculated incoherent tune spread is 0.62 to 0.16. Since the injected beam is small, with the average radius of 0.84 cm in the Booster, the beam can be injected significantly off-center both horizontally and vertically. This could result in as much as a factor of 2 reduction in the incoherent tune spread.

The off-centered transverse injection also results in the dilution of the transverse phase space. The beam emittance at the Booster exit can be expected to be several times larger than the injected beam. Present Booster beam with the Tandem injection of 40 turns usually has normalized horizontal and vertical 95% emittances of 6 and 3 $\pi \mu m$, or

8 and 4 times larger than the EBIS beam. Therefore, the Booster beam transverse emittance with the EBIS injection will not be a problem. In fact, emittance smaller than with Tandem beam injection can be expected, which may have a positive impact on the RHIC luminosity.

4.3 Longitudinal aspects

4.3.1 Capture of unbunched beam

The RF capture and the resultant longitudinal beam emittance are important issues. The present optimized scheme for the Tandem beam injection is to use an RF voltage of about 200V, with harmonic number of 6, at the $B = 0$ porch to capture the beam. The adiabatic-like capture takes about 6 ms. The resultant longitudinal emittance is $\sim 0.05 \text{ eVs}/u$ for the one Booster pulse (6 bunches). Once this beam becomes a RHIC bunch, the longitudinal emittance is enlarged to 0.3 to 0.4 eVs/u . Therefore, with the EBIS beam injection, the resultant Booster pulse longitudinal emittance should be not larger than 0.05 eVs/u .

The capture loss needs to be as small as possible. It is known that the lost beam may create a pressure increase, causing further beam loss.

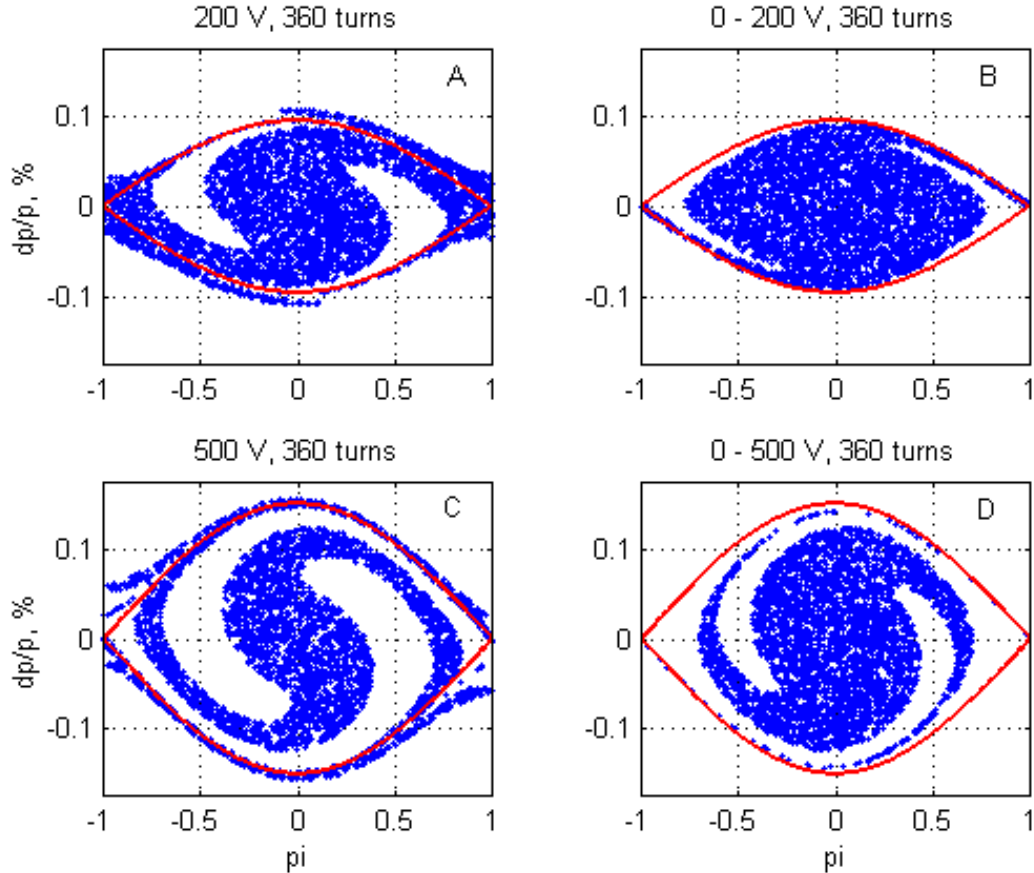


Fig 4.3.1.1 Simulation results for 4 different EBIS beam capture schemes

The injected beam momentum spread will have an impact on both aspects. Note that the Tandem beam momentum spread is very small, at about $\Delta\rho/\rho = \pm 0.01\%$. With the EBIS beam momentum spread of $\Delta\rho/\rho = \pm 0.05\%$ at the Booster injection, and much fewer turns injected, the injection scheme is substantially different from the existing one.

Simulation results for 4 different schemes of the EBIS beam capture are shown in Fig. 4.3.3.1. In the cases A and B, an RF voltage of 200V is used, but the latter is adiabatic type capture, i.e. the RF voltage is linearly increased from 0 V to 200 V in 360 turns, or 3.7 ms. The cases C and D are similar to the A and B, but the voltage is 500V. In Fig. 4.3.3.2, the mountain range of these captures is shown.

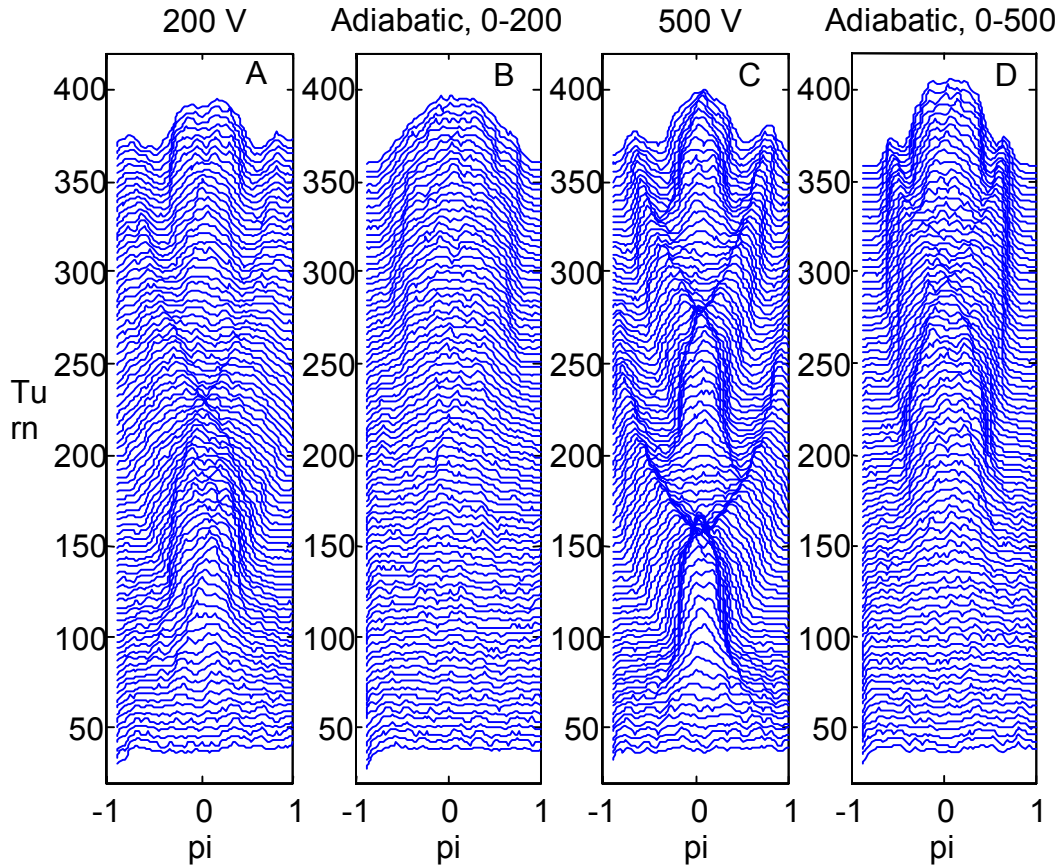


Fig. 4.3.3.2 Mountain range of 4 EBIS capture schemes

It can be observed that in the case B and D, all particles have been captured, and also the resultant emittance is relatively small. In fact, there is almost no emittance growth in the capture. Taking the case B as an example. The bucket area for $V_{RF} = 200$ V is $0.0083 eVs/u$. For a total of 6 buckets, the area is therefore $0.05 eVs/u$. It is seen from Fig. 4.3.3.1 that the bunch emittance is smaller than the bucket area, probably by 10% to 15%. On the other hand, the injected beam with the energy spread of $\pm 2keV/u$ and the pulse length of $10.3 \mu s$ gives rise to a total emittance of $0.041 eVs/u$, which is almost the same as the emittance of the captured beam.

The voltage amplitude of the Booster RF cavities, with the Band II full voltage of 35 kV, cannot be well controlled at low level. In fact, under 1.5 kV, counterphasing is needed to generate the required voltage. Therefore, the adiabatic capture requires some effort to be achieved. On the other hand, using constant voltage, the beam loss is still not significant, and the resultant beam emittance is not much larger. It also can be observed that the capture using 500 V RF voltage results in less beam loss, but larger diluted emittance, than the one with $V_{RF} = 200$ V.

Another issue at the injection is the possible longitudinal microwave instability with the EBIS beam. For the normalized emittance of $0.7 \pi \mu m$ and the injection energy of 2

MeV/u , the Booster longitudinal space charge impedance Z_l/n is $-j13.5k\Omega$. The peak EBIS beam current is about 6 mA. Using the Keil-Schnell criterion,

$$\left| \frac{\Delta p}{p} \right| > \sqrt{\frac{QeI_p}{4\gamma m_0 c^2 |\eta|} \left| \frac{Z_l}{n} \right|} \quad (2)$$

it is required that $|\Delta\rho/\rho| > 0.012\%$. This is satisfied by the EBIS injected beam with $|\Delta\rho/\rho| = \pm 0.005\%$.

We conclude that the beam longitudinal emittance requirement can be achieved. If further reduction of the longitudinal emittance is required, then smaller energy spread of the injected beam is needed.

4.3.2 Capture of bunched beam

With the potential capability of the EBIS to provide the bunched beam, it is of interest to look at this scenario, which requires no adiabatic capture. For the bunched beam capture, parameters shown in Table 4.3.2.1 are useful in choosing a proper injection scheme.

Table 4.3.2.1 Parameters for bunched beam capture

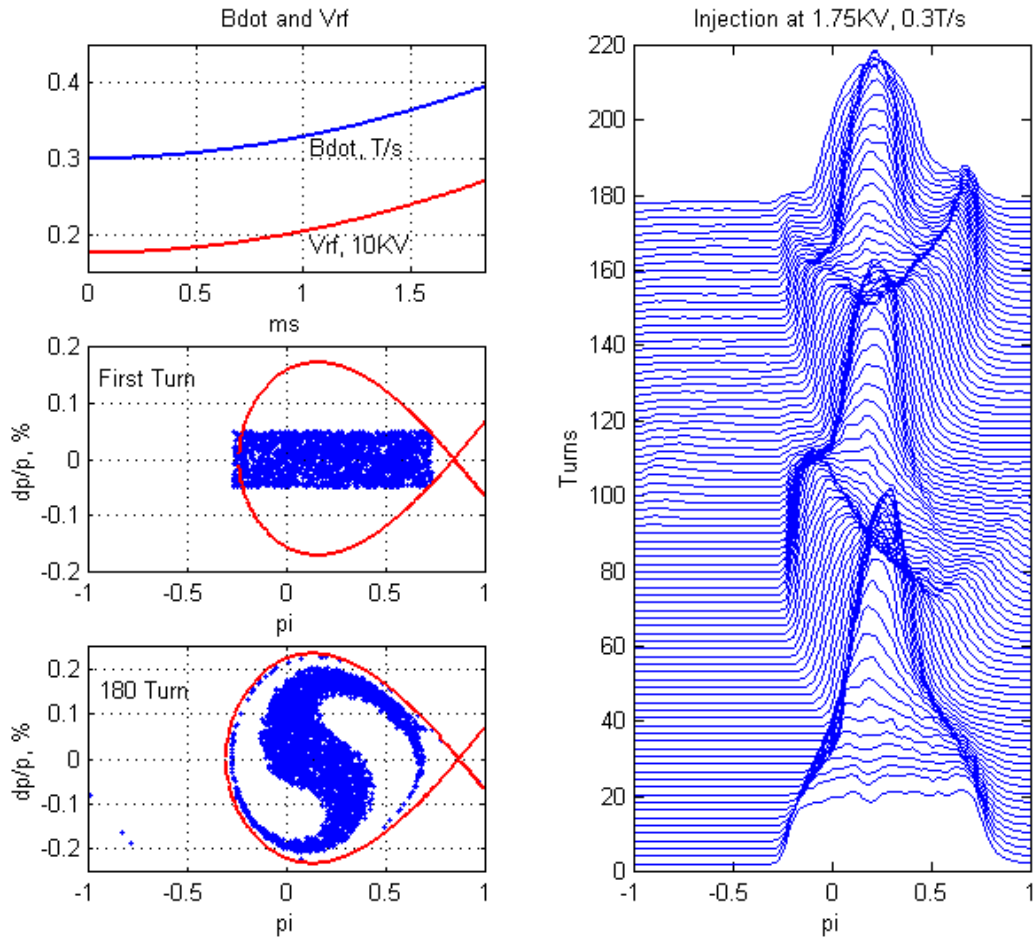
V_{RF}	\dot{B}	$\ell_{bk, ratio}$	$\Delta p / p_{bk}$	A_{bk}
2	0.1	0.78	0.27	0.0195
	0.3	0.58	0.19	0.0108
3	0.2	0.74	0.31	0.0218
	0.5	0.55	0.22	0.0118
5	0.5	0.67	0.35	0.0235
	1	0.49	0.23	0.0118
10	1	0.67	0.48	0.0332
	2	0.49	0.30	0.0167
15	2	0.61	0.48	0.0332
	3	0.49	0.34	0.0205
kV	T/s		%	eVs/u

The highest RF voltage available at the injection is about 15 kV, and the lowest RF voltage under good control is about 1.5 kV. The ratio of the moving bucket length over the RF period, $\ell_{bk, ratio}$ should be ≥ 0.5 , and the moving bucket area, A_{bk} , should be $\sim 0.01 eVs/u$, which implies total bucket area of $0.06 eVs/u$ for a Booster pulse. Also in the Table, $\Delta p / p_{bk}$ is the moving bucket half height in $\Delta p / p$.

It is indicated in Table 4.3.2.1 that the use of the RF voltage higher than 3 kV will result in either too large a bucket area or too small a bucket length. Therefore, 1.5 kV to 3 kV RF voltage with \dot{B} around $0.3 T/s$ might be a place to look.

In Fig. 4.3.2.1, we show an example with $V_{RF} = 1.75$ kV and $\dot{B} = 0.3 T/s$ at injection, with both V_{RF} and \dot{B} ramping up immediately following injection. On the left side, from top to the bottom, the V_{RF} and \dot{B} program, the particle in phase space of the first turn and turn 180, are shown. On the right side, the mountain range is shown. A small beam loss can be observed, however, it can be easily overcome by either reducing the injected bunch length, increasing the RF voltage, or reducing \dot{B} .

The resultant beam emittance is small; however, the reduction is from the smaller total emittance of the injected beam. Given the ratio of the bucket height to the beam momentum spread, some dilution exists. To better fit the beam into the bucket, lower RF voltage needs to be used.



4.4 Inflector Aperture Limit and Scraping Effect

The voltage required for the Booster C3 inflector is less than 50 kV for the EBIS beam injection, which is well within its operating range. The aperture of the inflector is 17 mm. Assuming the matched beam, then the horizontal β_H of the Booster at the inflector exit of $\beta_H = 11$ m gives rise to the full size of the injected beam, $2a = 2\sqrt{\varepsilon_{95} \beta_H} = 21.7\text{mm}$, which is slightly larger than the inflector aperture.

The window slit upstream of the inflector could be used to cut the beam transverse tail; however, without upgrade of the C3 inflector, beam scraping there is inevitable.

The most significant effect of the beam scraping is that the lost particles could generate a large number of ions and neutral particles, producing a local vacuum pressure bump. At the present Booster injection of $0.9\text{ MeV}/u$ gold beam with the loss of 2×10^9 ions, the pressure increased from $5 \times 10^{-11}\text{ Torr}$ to greater than $5 \times 10^{-8}\text{ Torr}$. The local vacuum pressure bump was longer than 10 meters in the Booster ring, in the vicinity of the exit of the C3 inflector. The circulating beam lifetime, therefore, was affected by the electron capture of the gold ions, and reduced from 200 ms to about 20 ms.

Given the much smaller amount of beam loss than the 2×10^9 ions, and also the fact that the sputtering effect is peaked below an energy of $1\text{ MeV}/u$, the vacuum pressure increase is expected to be much lower with the EBIS beam. An equally important factor is that the capture cross section at $2\text{ MeV}/u$ is much smaller than that at $0.9\text{ MeV}/u$. In Fig.4.4.1, the electron impact cross sections are shown. The capture cross section at $2\text{ MeV}/u$ is smaller than at $0.9\text{ MeV}/u$ by a factor of 40. Ionization will take place and become larger than electron capture only at $> 2.5\text{ MeV}/u$. We may expect, therefore, that the scraping of EBIS beam at the C3 inflector will have only a modest effect on the beam lifetime at injection.

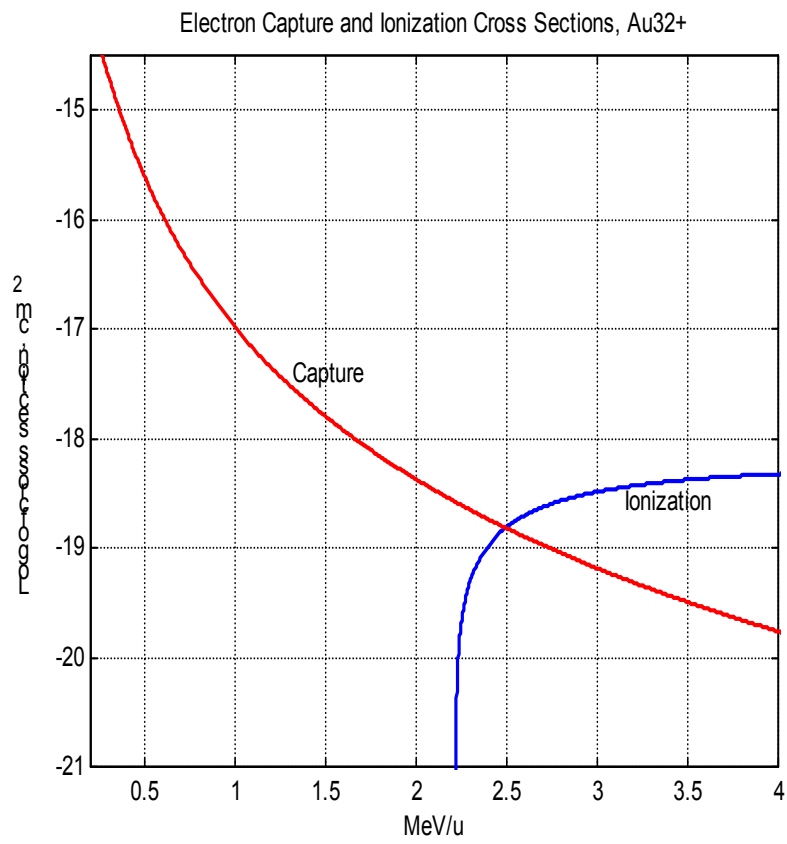
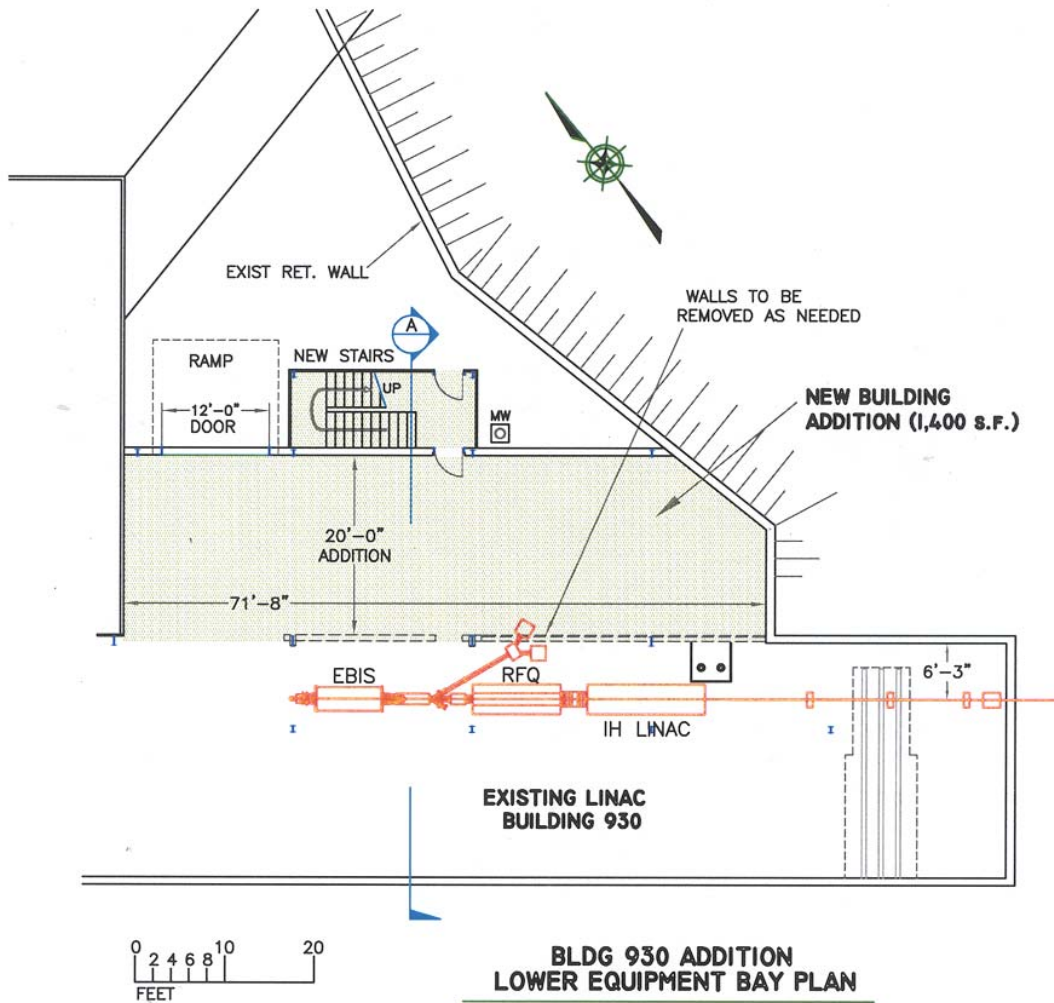


Fig. 4.4.1 Electron capture and ionization cross-sections, for Au³²⁺

5 Facility Modifications

The new preinjector will be housed in the lower equipment bay in Building 930 which contains the 200MeV Linac Facility. A two-story addition will be added to the building for supporting equipment. The HEBT line will enter the TTB line just before the electrostatic inflector via a new penetration through the Booster berm and concrete enclosed injection area. Figure 5.1 shows a layout of the preinjector in the new area. The addition is large enough to allow for future expansion, such as sources for polarized He³ or polarized deuterium injection, as well as space for EBIS improvements. Shielding will be required for the Linac and HEBT



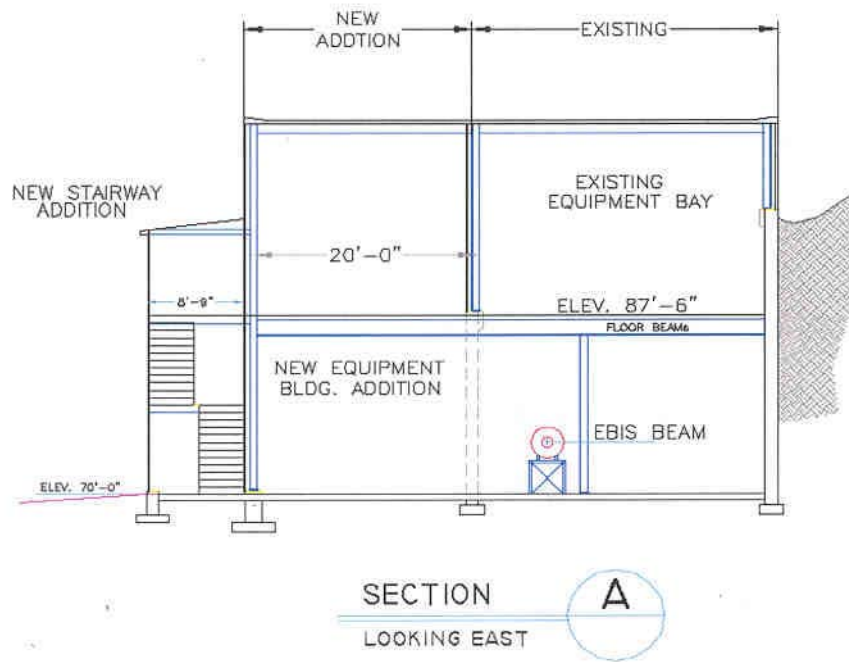


Fig. 5.1 Layout of the preinjector in the new building.

The facility modifications for the preinjector will provide approximately 2800 sq. ft. of new space, a 48 inch diameter, 10 foot long penetration through the lower equipment bay exterior wall and 12 inch diameter 30 foot long penetration into the Booster . The experimental space will house the EBIS, RFQ, linac, cooling systems, refrigerator, power supplies, and controls.

The Facility environments will be controlled by an efficient HVAC system designed to optimize energy conservation. The facility will be tied into the existing site wide Energy Management and Control System. The fire protection system will be hydraulically designed, in accordance with NFPA 13. Lighting levels and equipment will be designed to meet the latest DOE energy conservation requirements and to assure low maintenance costs. Laboratory environments will be monitored and recorded with appropriate alarms.

Sitework will include modifications and extension of the existing building, concrete walls to retain earth, and Trenching, excavation, backfilling as well as relocation, extensions, and connections to existing power, water, sanitary and storm sewers, alarm and telephone and computer networks will all be included.

6. ESHQ and Waste Management

The C-A Department maintains a formal Conduct of Operations agreement with the Department of Energy. The agreement requires C-a Department to execute its missions with procedures, chain-of-command supervision and qualified personnel. personnel are qualified in safe and environmentally responsible operations via an extensive training program that includes formal examinations where appropriate. The C-A Department will provide procedure management, environmental management, training and safety services to the staff associated with design, fabrication and operation of the Linac-Based RHIC Preinjector. The C-A Department will also prepare technical work products, and authorization documents, and provide waste management and assessment services to meet DOE requirements needed for authorized operation of the new Preinjector.

Operation of the Linac-Based RHIC Preinjector will produce industrial, hazardous and radioactive waste. At present, RHIC produces 25,000 lbs. of industrial waste , 400 lbs. of hazardous waste and about 100 cu. ft. of low-level radioactive waste each year. It is anticipated that waste from construction and operation of the Linac-based RHIC preinjector will be a small fraction of the present waste stream at RHIC. It is noted, however, that pollution prevention and waste minimization will be an integral part of the project and subsequent operation of the Preinjector.

References

- [2-1] A. Pikin, J. Alessi, E. Beebe, A. Kponou, K. Prelec, and L. Snyderstrup, *Rev. Sci. Instrum.* 69, 697 (1998).
- [2-2] A. Kponou, E. Beebe, A. Pikin, G. Kuznetsov, M. Batazova, and M. Tiunov, *Rev. Sci. Instrum.* 69, 1120 (1998).
- [2-3] A. Pikin, J. Alessi, E. Beebe, A. Kponou, K. Prelec, *Proc. PIBHI-2000, Conference Proceedings series of the Italian Physical Society.*
- [2-4] E. Beebe, J. Alessi, A. Kponou, A. Pikin, K. Prelec, *Proceedings of EPAC-2000, Vienna, Austria* p. 1589 (2000).
- [2-5] A. Kponou, E. Beebe, A. Pikin, G. Kuznetsov, M. Batazova, and M. Tiunov, *Rev. Sci. Instrum.* 69, 1120 (1998).
- [2-6] E.N. Beebe, J.G. Alessi, O. Gould, D. Graham, A. Kponou, A. Pikin, K. Prelec, J. Ritter, "Extraction of highly charged Au ions from a multiampere electron beam EBIS at BNL", *Rev. Sci. Instrum.* 73, 699 (2002).
- [2-7] A. Pikin, J. Alessi, E. Beebe, A. Kponou, K. Prelec, "Experimental study of ion injection into an extended trap of the Brookhaven National Laboratory EBIS", *Rev. Sci. Instrum.* 73, 670 (2002).
- [2-8] E. Beebe, J. Alessi, A. Kponou, A. Pikin, K. Prelec, "A New Generation of EBIS: High Current Devices for Accelerators and Colliders", *Proceedings of EPAC-2002, Paris, June 3-7, 2002*
- [2-9] A.I. Pikin, J.G. Alessi, E. Beebe, O. Gould, D. Graham, A. Kponou, K. Prelec, J. Ritter, V. Zajic, "Recent Results with Au Ions Extracted from an EBIS using an 8A Electron Beam at BNL", *Proceedings of EPAC-2002, Paris, June 3-7, 2002*
- [3-1] K.R. Crandall, R.H. Slokes, and T.P. Wangler, "RF Quadrupole beam dynamics studies", 1979 Linac Conf., BNL 51134, p. 205.
- [3-2] D. Raparia, "RFQ accelerator section and its optimization", 1988 Linac Conf., CEBAF-Report-89-001, p. 61.
- [3-3] U. Ratzinger and V.T. Mimje, "LORAS", description and manual

Appendix 1 Parameter List

EBIS

Solenoid length	1.5	m
Solenoid field	5.5 T	T
Electron beam current	10	A
Trap capacity	1.1e12	charges
Output (single charge state)	1.1e11	charges
Ion output (Au 32+)	3.4e9	particles/pulse
Pulse width	10-40	uS
Max rep rate	10	Hz
Beam current	1.7-0.42	mA
Output energy	8.5	keV/amu
Output emittance	0.35	pi mm mrad, norm, 90%

RFQ

Q/m	0.16 - 0.5	
Input energy	8.5	keV/amu
Output energy	300	keV/amu
Type	4 rod	
Frequency	100	MHz
Max rep rate	10	Hz
Length	2.96	m
Number of cells	236	
Aperture radius	0.006	m
Voltage	92	kV
E (surface)	20.8	MV/m
RF power (total)	< 350	kW
Acceptance	1.7	pi mm mrad
Input emittance	0.5	pi mm mrad, norm, 90%
Output emittance	0.5	pi mm mrad, norm, 90%
Output emittance (longit.)	0.75	pi MeV deg
Transmission	97%	

IH Linac

Q/m	0.16 - 0.5	
Input energy	300	keV/amu
Output energy	2000	keV/amu
Frequency	100	MHz
Max rep rate	10	Hz
Length	4	m
RF power (total)	< 350	kW
Input emittance	0.55	pi mm mrad, norm, 90%
Output emittance	7	pi mm mrad, norm, 90%
Output energy spread	+/- 20	keV/amu
Transmission	100%	

Transport line

dE after debuncher	+/- 2	keV/amu
Magnet/ps switching time	100	ms

Injection

# of turns injected	1-4	
Inflector voltage	44	kV
input match condition (at inflector)		
alphax	-1.73	
alphay	0.82	
betax	11.01	
betay	4.83	